The Plant Cell, Vol. 32: 1536–1555, May 2020, www.plantcell.org © 2020 ASPB.

A Tetratricopeptide Repeat Protein Regulates Carotenoid Biosynthesis and Chromoplast Development in Monkeyflowers (*Mimulus*)[OPEN]

Lauren E. Stanley,[a,1] Baoqing Ding,[a] Wei Sun,[b] Fengjuan Mou,[a,c] Connor Hill,[a] Shilin Chen,[b] and Yao-Wu Yuan[a,d,1]

[a] Department of Ecology and Evolutionary Biology, University of Connecticut, Storrs, Connecticut 06269
[b] Institute of Chinese Materia Medica, China Academy of Chinese Medical Sciences, Beijing 100700, China
[c] Faculty of Forestry, Southwest Forestry University, Kunming, Yunnan 650224, China
[d] Institute for Systems Genomics, University of Connecticut, Storrs, Connecticut 06269

ORCID IDs: 0000-0001-9579-0639 (L.E.S.); 0000-0001-7183-9653 (B.D.); 0000-0001-5675-0466 (W.S.); 0000-0002-4134-3128 (F.M.); 0000-0003-4114-4513 (C.H.); 0000-0002-0449-236X (S.C.); 0000-0003-1376-0028 (Y.-W.Y.)

Little is known about the factors regulating carotenoid biosynthesis in flowers. Here, we characterized the *REDUCED CAROTENOID PIGMENTATION2* (*RCP2*) locus from two monkeyflower (*Mimulus*) species, the bumblebee-pollinated species *Mimulus lewisii* and the hummingbird-pollinated species *Mimulus verbenaceus*. We show that loss-of-function mutations of *RCP2* cause drastic down-regulation of the entire carotenoid biosynthetic pathway. The causal gene underlying *RCP2* encodes a tetratricopeptide repeat protein that is closely related to the Arabidopsis (*Arabidopsis thaliana*) REDUCED CHLOROPLAST COVERAGE proteins. RCP2 appears to regulate carotenoid biosynthesis independently of RCP1, a previously identified R2R3-MYB master regulator of carotenoid biosynthesis. We show that RCP2 is necessary and sufficient for chromoplast development and carotenoid accumulation in floral tissues. Simultaneous down-regulation of *RCP2* and two closely related paralogs, *RCP2-L1* and *RCP2-L2*, yielded plants with pale leaves deficient in chlorophyll and carotenoids and with reduced chloroplast compartment size. Finally, we demonstrate that *M. verbenaceus* is just as amenable to chemical mutagenesis and in planta transformation as the more extensively studied *M. lewisii*, making these two species an excellent platform for comparative developmental genetics studies of closely related species with dramatic phenotypic divergence.

INTRODUCTION

The colors of most flowers can be attributed to two classes of pigments: the red, pink, purple, or blue anthocyanins and the yellow, orange, or red carotenoids. The hydrophilic anthocyanins are usually stored in the vacuoles of petal cells, whereas the hydrophobic carotenoids accumulate in chromoplasts as various lipoprotein structures (e.g., plastoglobules, crystals, fibrils; Grotewold and Davies, 2008; Egea et al., 2010; Li and Yuan, 2013). A plant can frequently produce both pigment types in the same flower, forming contrasting spatial patterns that serve as nectar guides for animal pollinators (Glover, 2014). Common examples among horticultural plants include pansies (*Viola tricolor*), primroses (*Primula vulgaris*), lantanas (*Lantana camara*), and hibiscus (*Hibiscus rosa-sinensis*), to name but a few. As an example in nature, the vast majority of the ~160 species of monkeyflowers (*Mimulus*; Barker et al., 2012) produce both anthocyanins and carotenoids in their petals with striking patterns. While most plant genomes contain the genes encoding both anthocyanin and carotenoid biosynthetic pathways, the diversity of floral pigmentation patterns is largely due to when and where these pathway genes are expressed. As such, identifying the transcriptional regulators of these pigment biosynthetic pathways is critically important to understanding the developmental mechanisms of pigment pattern formation and the molecular bases of natural flower color variation.

The transcriptional control of anthocyanin biosynthesis is well understood. A highly conserved MYB-bHLH-WD40 (MBW) protein complex has been shown to coordinately activate all or some of the anthocyanin biosynthetic pathway genes in multiple plant systems (Paz-Ares et al., 1987; Ludwig et al., 1989; Martin et al., 1991; Goodrich et al., 1992; de Vetten et al., 1997; Quattrocchio et al., 1998; Borevitz et al., 2000; Spelt et al., 2000; Schwinn et al., 2006; reviewed by Davies et al., 2012; Xu et al., 2015). Among the three components, members of the R2R3-MYB transcription factor family often display tissue-specific expression patterns and cause spatial patterning of anthocyanin deposition in flower petals (Shang et al., 2011; Albert et al., 2011; Yuan et al., 2014; Martins et al., 2017).

By contrast, little is known about the transcriptional regulators of the carotenoid biosynthetic pathway (CBP) in flowers (Ruiz-Sola and Rodríguez-Concepción, 2012; Yuan et al., 2015), although many putative transcriptional regulators have been identified in other tissues. For example, in Arabidopsis leaves, PHYTOCHROME-INTERACTING FACTOR1 (PIF1) and ELONGATED HYPOCOTYL5 (HY5) operate as a regulatory switch during

[1] Address correspondence to lauren.stanley@uconn.edu and yuan.colreeze@gmail.com.
The authors responsible for distribution of materials integral to the findings presented in this article in accordance with the policy described in the Instructions for Authors (www.plantcell.org) are: Lauren E. Stanley (lauren.stanley@uconn.edu) and Yao-Wu Yuan (yuan.colreeze@gmail.com).
[OPEN]Articles can be viewed without a subscription.
www.plantcell.org/cgi/doi/10.1105/tpc.19.00755

IN A NUTSHELL

Background: Carotenoids are yellow, orange, or red pigments that give many flowers and fruits their brilliant colors. In order to make and accumulate carotenoids in these organs, plants must (i) switch on the genes for carotenoid-producing enzymes and (ii) build specialized storage organelles called chromoplasts. However, very few regulatory genes controlling these two processes in flowers have been identified.

Question: We wanted to discover new regulators of carotenoid production and storage in flowers. We did this by chemically mutating the DNA of two species of *Mimulus* (monkeyflower) and searching for mutants lacking yellow pigmentation in their flowers. We sequenced the DNA of one mutant with a dramatic decrease in carotenoid accumulation to identify which gene was impaired and did experiments to characterize how this gene contributes to flower coloration.

Findings: We found a gene that we named *REDUCED CAROTENOID PIGMENTATION2* (*RCP2*), because disruption of this gene causes *Mimulus* flowers to lose most of their carotenoids. *rcp2* mutant plants cannot switch on carotenoid enzyme genes to the same degree as wild-type plants and do not make normal chromoplast storage organelles. When we engineered plants to make extra RCP2 proteins, the normally whitish floral reproductive organs turned yellow. Together, these results show that RCP2 is necessary and sufficient for carotenoid pigmentation in *Mimulus* flowers. Interestingly, although *RCP2* by itself has no effect on carotenoid accumulation in leaves, simultaneously turning down the expression of *RCP2* and two closely related genes (*RCP2-like* genes) resulted in pale leaves that were deficient in both carotenoid and chlorophyll pigments and with a smaller cell volume occupied by chloroplasts. This indicates that the original function of *RCP2-like* genes might have been to regulate essential chlorophyll and carotenoid pigments in vegetative tissues and that *RCP2* has evolved specialized function in the regulation of carotenoid accumulation in reproductive organs for pollinator attraction.

Next steps: Moving forward, we want to learn more about the functional mechanism of RCP2 by identifying proteins that physically interact with RCP2 and to discover additional carotenoid regulators in the monkeyflower system by analyzing chemically induced mutants and natural variation.

photomorphogenesis, binding to the promoter of the phytoene synthase gene *PSY* to repress and activate carotenoid biosynthesis, respectively (Toledo-Ortiz et al., 2010, 2014). Another regulator, RELATED TO AP2 2 (RAP2.2), binds the promoters of *PSY* and the phytoene desaturase gene *PDS* in vitro, although its endogenous function in leaf carotenoid regulation remains unclear (Welsch et al.,2007). In addition, the histone methyltransferase SET DOMAIN GROUP8 (SDG8) activates the transcription of the carotenoid isomerase gene *CRTISO* by altering the methylation status around the transcription start site of this gene (Cazzonelli et al., 2009).

Numerous putative transcriptional regulators of carotenoid biosynthesis have also been described in fruits, particularly tomatoes (*Solanum lycopersicum*). For example, the MADS-box proteins RIPENING INHIBITOR (RIN), FRUITFULL1 (FUL1) and FUL2, TOMATO AGAMOUS LIKE1 (TAGL1), and SlMADS1 are master regulators of fruit ripening. Each protein regulates a subset of CBP genes, cooperatively promoting the production of lycopene, the major carotenoid in tomato fruits (Vrebalov et al., 2002; Ito et al., 2008; Itkin et al., 2009; Vrebalov et al., 2009; Giménez et al., 2010; Fujisawa et al., 2011, 2012, 2013, 2014; Martel et al., 2011; Bemer et al., 2012; Qin et al., 2012; Dong et al., 2013; Shima et al., 2013; Zhong et al., 2013). However, as these master regulators are involved in other aspects of fruit ripening (e.g., softening, aroma, and sugar production), it is difficult to decipher their specific functions in carotenoid regulation. Other classes of carotenoid regulators during tomato fruit ripening include SlNAC1/4, SlAP2a, and SlBBX20 (Chung et al., 2010; Karlova et al., 2011; Ma et al., 2014; Zhu et al., 2014; Meng et al., 2016; Xiong et al., 2019). Interestingly, SlPIF1a appears to play a similar role in carotenoid regulation at the onset of fruit ripening as its Arabidopsis homolog AtPIF1 does in photomorphogenesis by repressing the expression of *SlPSY1* until chlorophyll degradation (Llorente et al., 2016). Putative carotenoid transcriptional regulators have also been identified in other fruits, including CsMADS6 and CrMYB68 in orange (*Citrus* spp; Zhu et al., 2017; Lu et al., 2018), CpEIN3a, CpNAC1, CpNAC2, CpbHLH1, and CpbHLH2 in papaya (*Carica papaya*; Fu et al., 2016, 2017; Zhou et al., 2019), and AdMYB7 in kiwifruit (*Actinidia deliciosa*; Ampomah-Dwamena et al., 2019).

However, whether these leaf or fruit carotenoid regulators play a role in flower pigmentation is unknown. To date, only two transcriptional regulators have been implicated in carotenoid pigmentation in flower petals. *REDUCED CAROTENOID PIGMENTATION1* (*RCP1*), identified from the monkeyflower species *Mimulus lewisii*, encodes a subgroup-21 R2R3-MYB (Sagawa et al., 2016). The ventral (lower) petal of *M. lewisii* flowers contains two yellow ridges that are pigmented by carotenoids (Figure 1A), which serve as nectar guides for bumblebee pollinators (Owen and Bradshaw, 2011). Loss-of-function mutations in *RCP1* reduce the expression of the entire CBP and decrease the carotenoid content in the nectar guides (Figure 1B; Sagawa et al., 2016). *WHITE PETAL1* (*WP1*), identified from *Medicago truncatula*, encodes a subgroup-6 R2R3-MYB (Meng et al., 2019). Loss-of-function *wp1* mutants show dramatically reduced carotenoid contents and down-regulation of multiple carotenoid biosynthetic genes in flower petals. Since subgroup-6 R2R3-MYBs typically activate anthocyanin biosynthesis in plants (Davies et al., 2012; Glover, 2014; Xu et al., 2015), *WP1* represents an intriguing case where an anthocyanin activator

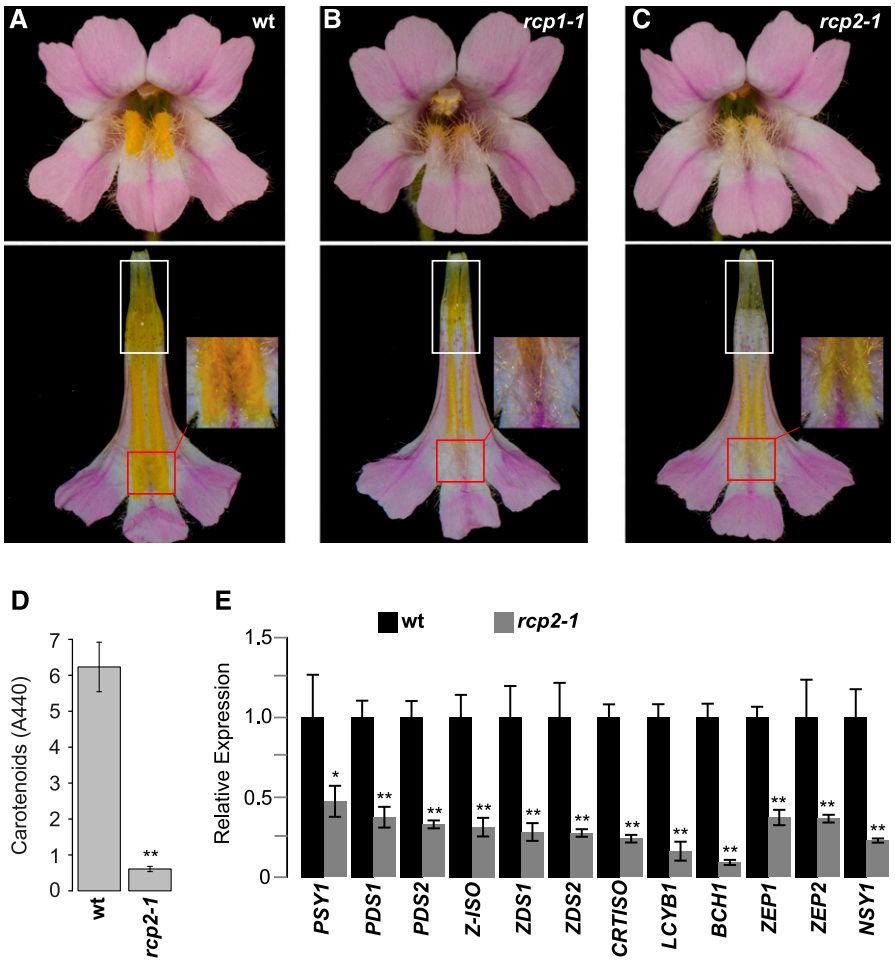

Figure 1. Reduced Carotenoid Pigmentation Phenotypes in *M. lewisii*.

Front view (top) and nectar guide view (bottom) of wild-type **(A)**, *rcp1-1* **(B)**, and *rcp2-1* **(C)** flowers. White and red boxes indicate the base and throat of the corolla tube, respectively.

(D) Carotenoid concentrations in wild-type and *rcp2-1* nectar guides, approximated based on absorbance measurements at 440 nm. Error bars are 1 SD ($n = 8$ individual flowers from the same plant).

(E) Relative transcript levels of the CBP genes in 15-mm nectar guides of wild-type and *rcp2-1* flowers, as determined by qRT-PCR. Error bars are 1 SD ($n = 3$ biological replicates, each consisting of pooled 15-mm nectar guides from a distinct plant). Asterisks indicate differences from the wild type (*$P < 0.05$, **$P < 0.01$, Student's t test).

might have been co-opted to regulate carotenoid pigmentation in some exceptional lineages. Besides these R2R3-MYBs, the carotenoid cleavage dioxygenases (particularly CCD1 and CCD4s) are well-known contributors to flower color variation among species or horticultural varieties that modulate carotenoid turnover (Ohmiya et al., 2006; Chiou et al., 2010; Zhang et al., 2015), although they are not involved in transcriptional regulation of the CBP per se.

In this study, to identify additional transcriptional regulators of floral carotenoid pigmentation, we characterized *reduced carotenoid pigmentation 2* (*rcp2*) mutants in *Mimulus*. Through bulk segregant analysis and transgenic experiments, we identified the causal gene of *RCP2*, encoding a tetratricopeptide repeat (TPR) protein homologous to the REDUCED CHLOROPLAST COVERAGE (REC) proteins in Arabidopsis. Loss-of-function *REC* mutants have reduced chlorophyll contents and smaller chloroplast compartment size compared with wild type (Larkin et al., 2016). Our analyses showed that *RCP2* is required for chromoplast development and carotenoid biosynthesis in *Mimulus* flowers and that overexpression of *RCP2* in pale or colorless floral tissues (e.g., filaments, style) promotes chromoplast formation and carotenoid accumulation. Additionally, we demonstrate that simultaneous down-regulation of *RCP2* and its two closely related paralogs reduces leaf chlorophyll and carotenoid contents as well as chloroplast coverage in *Mimulus*, suggesting that this small family of TPR genes plays conserved roles in regulating chlorophyll accumulation and chloroplast compartment size in eudicots.

RESULTS

rcp2-1 Displays a Distinct and Stronger Phenotype Than *rcp1-1*

We recovered three independent *rcp2* alleles from an ethyl methanesulfonate (EMS) mutant screen in the *M. lewisii* LF10 background. *rcp2-1* and *rcp2-2* are very similar phenotypically, whereas *rcp2-3* displays a slightly weaker phenotype (Figure 1C; Supplemental Figure 1). Like the *rcp1-1* mutant, *rcp2-1* has reduced carotenoid contents in the nectar guides compared to the wild type. However, *rcp2-1* can be readily distinguished from *rcp1-1* in two ways. First, the total carotenoid content in the nectar guides of *rcp2-1* is ~10-fold lower than the wild type (Figure 1D), whereas that of *rcp1-1* is only ~4.4-fold lower (Sagawa et al., 2016). Second, the residual carotenoid pigments in *rcp1-1* and *rcp2-1* show distinct spatial distributions. At the base of the corolla tube (white boxes in Figures 1A to 1C), carotenoid pigments are completely lacking in *rcp2-1* but present in *rcp1-1*. By contrast, at the throat of the corolla tube (red boxes in Figures 1A to 1C), carotenoid pigments are completely lacking in *rcp1-1* but present at low concentrations in *rcp2-1*, giving a cream instead of bright yellow color. These spatial distribution patterns of residual pigments are consistent among allelic mutants within each complementation group (Supplemental Figure 1).

To test whether RCP2 regulates CBP genes at the transcriptional level, we performed qRT-PCR experiments on nectar guide tissue at the 15-mm corolla developmental stage (same stage as in the previous study on *RCP1*; Sagawa et al., 2016). Compared with wild type, the *rcp2-1* mutant showed a coordinated down-regulation of the entire CBP (Figure 1E), with a 3- to 4-fold decrease in expression of most CBP genes and ~10-fold decrease in *BETA CAROTENOID HYDROXYLASE1* (*BCH1*) expression. These results suggest that RCP2 is involved in the transcriptional regulation of CBP genes in the nectar guides. Consistent with the more severe reduction in total carotenoid content, the extent of CBP gene down-regulation is stronger in *rcp2-1* than in *rcp1-1* (Sagawa et al., 2016).

In contrast to the wholesale CBP down-regulation in the nectar guides, only two CBP genes (*ZDS2* and *ZEP1*) showed >1.5-fold down-regulation (with $P < 0.05$) in *rcp2-1* leaf tissue (Supplemental Figure 1; Supplemental Data Set 1).

Two Additional *rcp2* Mutants Are Recovered from *Mimulus verbenaceus*

Coincidentally, we found two additional *rcp2* mutants in *M. verbenaceus*, a hummingbird-pollinated species that is closely related to *M. lewisii* (Beardsley et al., 2003). We performed a pilot EMS mutagenesis experiment using the *M. verbenaceus* inbred line MvBL as part of our effort to develop these two species as a platform for comparative developmental genetics studies. We screened 460 M2 families (~20 M2 plants per family) and recovered more than 100 floral mutants. While wild-type *M. verbenaceus* (MvBL) produces bright red corollas with high concentrations of yellow carotenoids and magenta anthocyanins (Figure 2A), two recessive mutants (*MV00025* and *MV00051*) lack

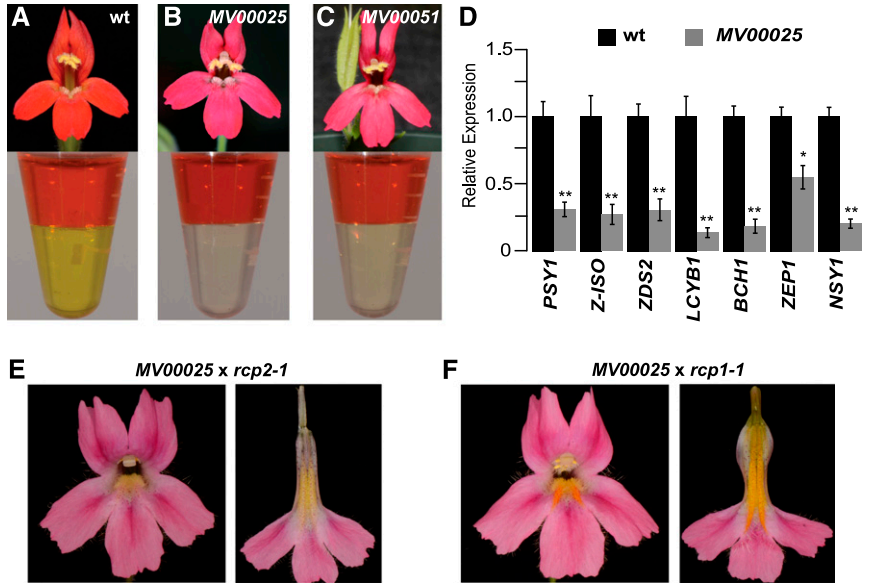

Figure 2. *rcp2* Phenotypes in *M. verbenaceus* Flowers.

Phenotypes of wild-type **(A)**, *MV00025* **(B)**, and *MV00051* **(C)** flowers. Top row, Front view of the flower. Bottom row, Separation of anthocyanins (top aqueous layer) and carotenoids (bottom organic layer).

(D) qRT-PCR of a subset of the CBP genes in wild-type *M. verbenaceus* and *MV00025*. Error bars are 1 SD ($n = 3$ biological replicates, each consisting of pooled 15-mm corollas from a distinct plant); asterisks indicate differences from the wild type (*$P < 0.05$, **$P < 0.01$, Student's *t* test).

(E) and **(F)** Complementation crosses between *MV00025* and *M. lewisii rcp2* and *rcp1* mutants.

carotenoids in the entire corolla (Figures 2B and 2C). Similar to *M. lewisii rcp2-1*, the *M. verbenaceus* mutants show coordinated down-regulation of CBP genes compared with wild-type MvBL (Figure 2D).

Crossing these two mutants with each other and with *M. lewisii rcp2-1* produced plants bearing flowers with very little carotenoid pigmentation in the nectar guides (Figure 2E). By contrast, crosses between the *M. verbenaceus* mutants and *rcp1-1* produced plants with intense yellow color in the nectar guides (Figure 2F). These complementation crosses suggest that *MV00025* and *MV00051* represent two additional *rcp2* alleles. Note that the F1 hybrids between *M. lewisii* and *M. verbenaceus* have pink petal lobes without carotenoids because they are heterozygous for *YELLOW UPPER* (*YUP*), a dominant repressor known to prevent carotenoid

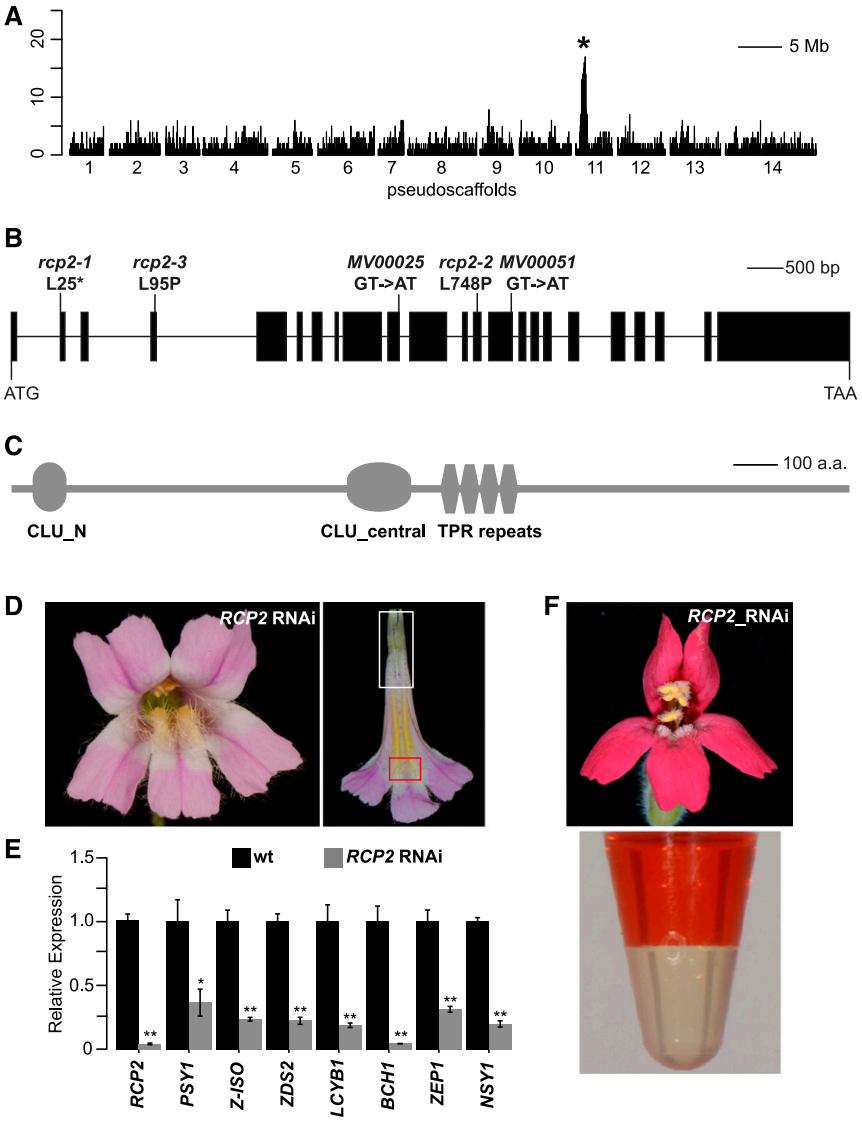

Figure 3. Identification of *RCP2*.

(A) Whole-genome scan for regions enriched in homozygous SNPs.
(B) Schematic *RCP2* gene map highlighting mutations from *M. lewisii (rcp2-1*, *rcp2-2*, *and rcp2-3)* and *M. verbenaceus* (*MV00025* and *MV00051*). Black boxes, exons; lines, introns.
(C) RCP2 protein schematic showing the key domains.
(D) Front view and nectar guide view of a representative *M. lewisii RCP2* RNAi line. White and red boxes indicate the base and throat of the corolla tube, respectively.
(E) Relative transcript levels of a subset of CBP genes in 15-mm nectar guides of *M. lewisii RCP2* RNAi lines compared to the wild type, as determined by qRT-PCR. Error bars are 1 SD ($n = 3$ biological replicates, each consisting of pooled 15-mm nectar guides from an independent RNAi line); asterisks indicate differences from the wild type (*$P < 0.05$, **$P < 0.01$, Student's t test).
(F) Front view (top) and pigment separation (bottom) of a representative *RCP2* RNAi flower in *M. verbenaceus*.

accumulation in the petal lobes (Hiesey et al., 1971): *M. lewisii* is homozygous for the dominant allele and *M. verbenaceus* is homozygous recessive.

RCP2 Encodes a TPR Protein

To identify *RCP2*, we performed bulk segregant analysis by Illumina sequencing of an F2 population, which was derived from a cross between *rcp2-1* (in the LF10 background) and the mapping line SL9 (see Methods). A conspicuous peak was detected on pseudoscaffold 11 (Figure 3A), corresponding to a 70-kb region in the LF10 genome (LF10g_v1.8 scaffold 278, 1,215,000 to 1,285,000). Remapping the Illumina reads to this 70-kb interval of the LF10 genome revealed only one mutation in the entire region. This mutation causes a premature stop codon at the beginning of the second exon of a gene encoding a TPR protein of 1794 amino acids (Figure 3B), with a calculated mass of 196 kD. Sequencing the independent *rcp2-2* and *rcp2-3* alleles showed that both contain nonsynonymous amino acid replacements at highly conserved sites (Figure 3B; Supplemental Figure 2) of this TPR protein. Additionally, *MV00025* and *MV00051* each contain an intron splicing mutation in this gene (Figure 3B), corroborating the results of the complementation test.

To further verify that this *TPR* gene is *RCP2*, we knocked down its expression in both species, expecting to recapitulate the mutant phenotypes. To this end, we constructed an RNA interference (RNAi) plasmid using a 408-bp fragment in the last exon of the *M. lewisii TPR* gene, which has a unique nucleotide sequence, as determined by BLAST analysis against the LF10 genome assembly, and transformed it into wild-type LF10. We

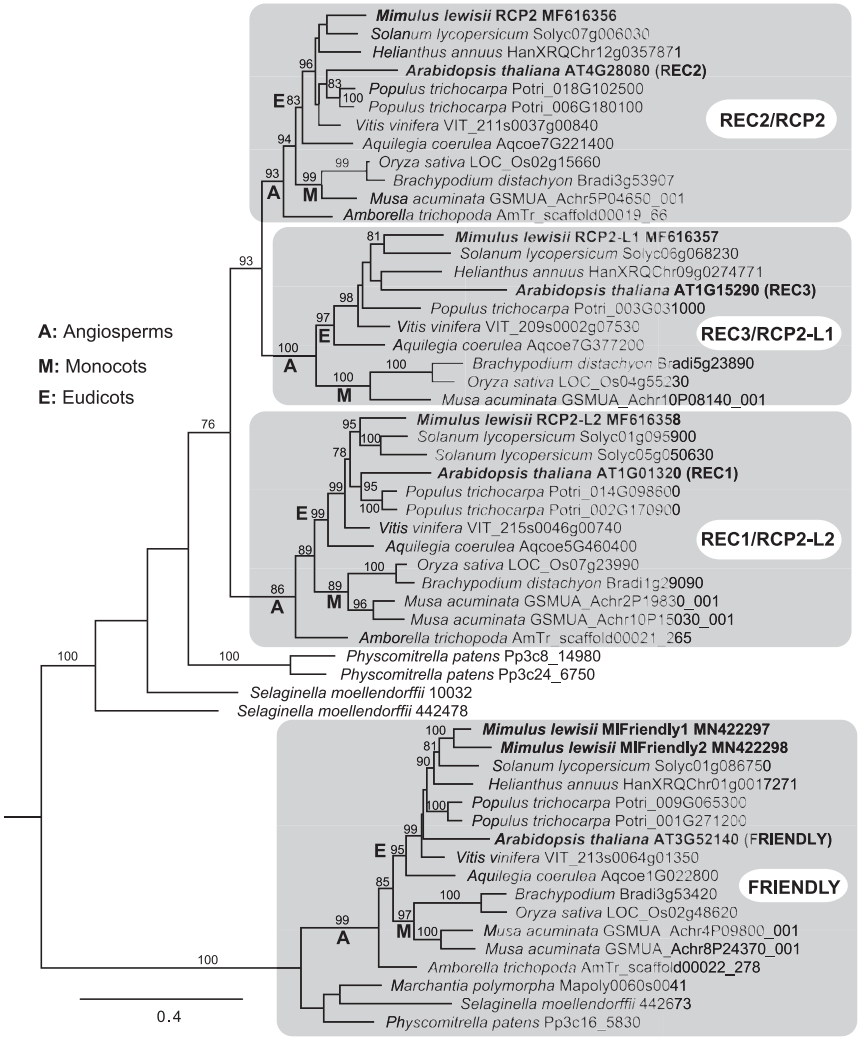

Figure 4. Maximum Likelihood (ML) Phylogenic Tree of RCP2 and Related Proteins.

GenBank accession numbers for the *Mimulus* sequences are provided after each gene name. The Arabidopsis sequences were retrieved from TAIR (https://www.arabidopsis.org/). All other sequences were retrieved from Phytozome v13 (https://phytozome-next.jgi.doe.gov/), with locus name following the species name. Bootstrap values higher than 75 are shown along the branches. The tree was rooted by midpoint rooting. "A," "M," and "E" indicate the clades containing all angiosperms, monocots, and eudicots, respectively.

obtained 127 stable transgenic plants, 96% of which closely resemble the *rcp2-1* mutant, including the complete lack of yellow pigments at the base of the corolla tube and the creamy yellow color at the throat of the corolla tube (Figure 3D). Evaluation of the expression level of this *TPR* gene in three of the RNAi lines showed ~95% knockdown, and qRT-PCR confirms that the CBP genes are also down-regulated in the RNAi lines to a similar degree as in the *rcp2-1* mutant (Figure 3E). Transforming the same RNAi construct into MvBL (the RNAi fragment has 95% sequence identity between the two species) yielded 40 independent transgenic lines, 37 of which recapitulated the mutant phenotype (Figure 3F). Based on the bulk segregant analysis, five independent allelic mutants, and the RNAi results, we conclude that this *TPR* gene is indeed *RCP2* and that *rcp2-1* is likely to be a null allele, as the translated protein would contain only 24 of the 1794 amino acids (Figure 3B).

BLAST analysis of the RCP2 protein sequence against the NCBI Conserved Domain Database (Marchler-Bauer et al., 2015) revealed three conserved domains—a TPR domain with four TPR repeats, a CLUstered mitochondria protein N-terminal domain (CLU_N), and a CLU central domain (CLU_central; Figure 3C)—but no recognizable DNA binding domain. TPR repeats, which are found in a wide range of proteins, function as scaffolds to mediate protein-protein interactions (D'Andrea and Regan, 2003; Zeytuni and Zarivach, 2012; Bohne et al., 2016). By contrast, no specific functions have been assigned to the CLU domains to date. There are two closely related paralogs of *RCP2* in the *M. lewisii* genome, *RCP2-L1* and *RCP2-L2* (Figure 4; Supplemental Figure 2). Phylogenetic analysis indicates that the divergence of these three paralogs predated the origin of angiosperms: there is a corresponding ortholog for each of the three genes in both eudicots and monocots as well as the most basal angiosperm lineage, *Amborella* (note that the lack of *RCP2-L1*/*REC3* ortholog in *Amborella* is most likely due to secondary loss; Figure 4). The Arabidopsis homologs (*REC1*, *AT1G01320*; *REC2*, *AT4G28080*; *REC3*, *AT1G15290*) help establish the size of the chloroplast compartment in Arabidopsis leaf cells (Larkin et al., 2016). All the *REC* genes together are sister to the *FRIENDLY* clade (Figure 4), as shown in Larkin et al. (2016).

The existence of three closely related paralogs with potentially redundant functions raised the question as to why mutations in a single gene, *RCP2*, result in such a strong phenotype in floral carotenoid pigmentation. We hypothesized that *RCP2* and the *RCP2*-like genes have evolved different expression patterns. To test this, we performed RT-PCR at different stages of LF10 corolla development and in different tissues. *RCP2* is primarily expressed in the corolla (both nectar guides and petal lobes) and its expression gets progressively stronger as the corolla grows larger and the yellow color in the nectar guides becomes more intense (Figures 5A to 5C). By contrast, *RCP2-L1* and *RCP2-L2* are only expressed in the early stages of corolla development before the yellow color becomes conspicuous, suggesting these genes play a relatively minor role in floral carotenoid pigmentation compared to *RCP2*. On the other hand, these two genes are strongly expressed in the leaf, where *RCP2* is expressed relatively weakly.

RCP2 Is Required for Chromoplast Development

The *RCP2* homologs in Arabidopsis, *REC1* to *REC3*, are involved in controlling the chloroplast compartment size (Larkin et al., 2016), and the gene that is sister to the *REC* clade, *FRIENDLY* (Larkin et al., 2016), controls mitochondrial morphology and intracellular distribution (Logan et al., 2003; El Zawily et al., 2014). These observations prompted us to investigate the possibility that *RCP2* is involved in the development of another organelle, the chromoplast, in *Mimulus* flowers. This supposition seemed promising because chromoplasts and chloroplasts are known to be interconvertible (Egea et al., 2010; Li and Yuan, 2013), and chromoplast development is known to play an important role in carotenoid accumulation, although not necessarily in the global

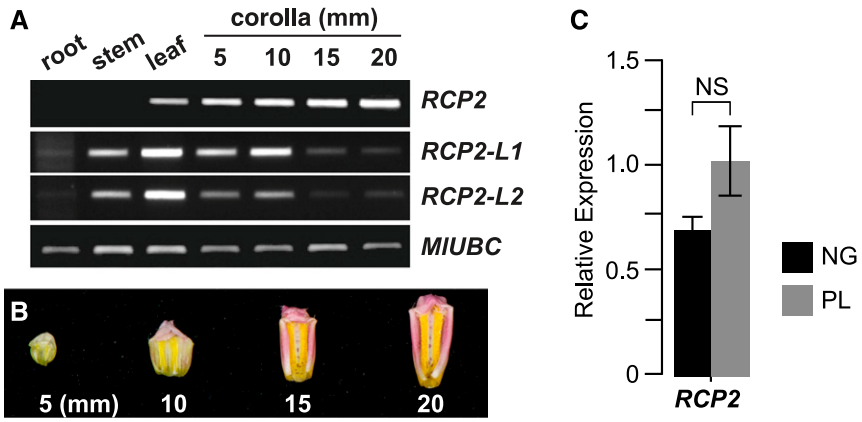

Figure 5. Expression Patterns of *RCP2*, *RCP2-L1*, and *RCP2-L2*.

(A) Qualitative RT-PCR (28 cycles) of *RCP2* and *RCP2-like* genes in various tissues and corollas at different developmental stages in wild-type *M. lewisii.* Root, stem, and leaf tissues were collected from 4-week old seedlings. *MIUBC* was used as the reference gene.

(B) Carotenoid accumulation in the nectar guides of wild-type *M. lewisii* across developmental stages.

(C) qRT-PCR measurement of relative *RCP2* expression level in *M. lewisii* nectar guides (NG) and petal lobes (PL). Error bars are 1 SD ($n = 3$ biological replicates, each consisting of pooled 15-mm nectar guides (NG) or petal lobes (PL) from a distinct plant. NS, non-significant; Student's *t* test).

transcriptional regulation of CBP genes (Mustilli et al., 1999; Liu et al., 2004a; Lu, 2006; Galpaz et al., 2008; Lopez et al., 2008; Chayut, 2017). To test this possibility, we examined the ultrastructure of flower epidermal cells by transmission electron microscopy (TEM). In wild-type *M. lewisii* nectar guide epidermal cells, numerous rounded chromoplasts are pushed to the periphery of the cell by the vacuole (Figure 6A), and each chromoplast contains several electron-dense plastoglobuli, the main carotenoid-sequestering structures (Figure 6B). In sharp contrast, in the *rcp2* mutant, the chromoplasts on the cell periphery are skinny, irregularly shaped, and usually contain few plastoglobuli (Figures 6C and 6D). Similar differences can be observed in *MV00025* petal lobe epidermal cells compared with wild-type MvBL (Figures 6E and 6F). These results suggest that *RCP2* is required for proper chromoplast development.

Because carotenoid accumulation is concomitant with chromoplast formation, it is difficult to distinguish whether the malformation of chromoplasts disrupts the transcription of the carotenoid biosynthesis genes or whether a lack of carotenoids due to the down-regulation of the CBP genes leads to the improper development of chromoplasts. We reasoned that if decreased carotenoid biosynthesis causes the chromoplast malformation,

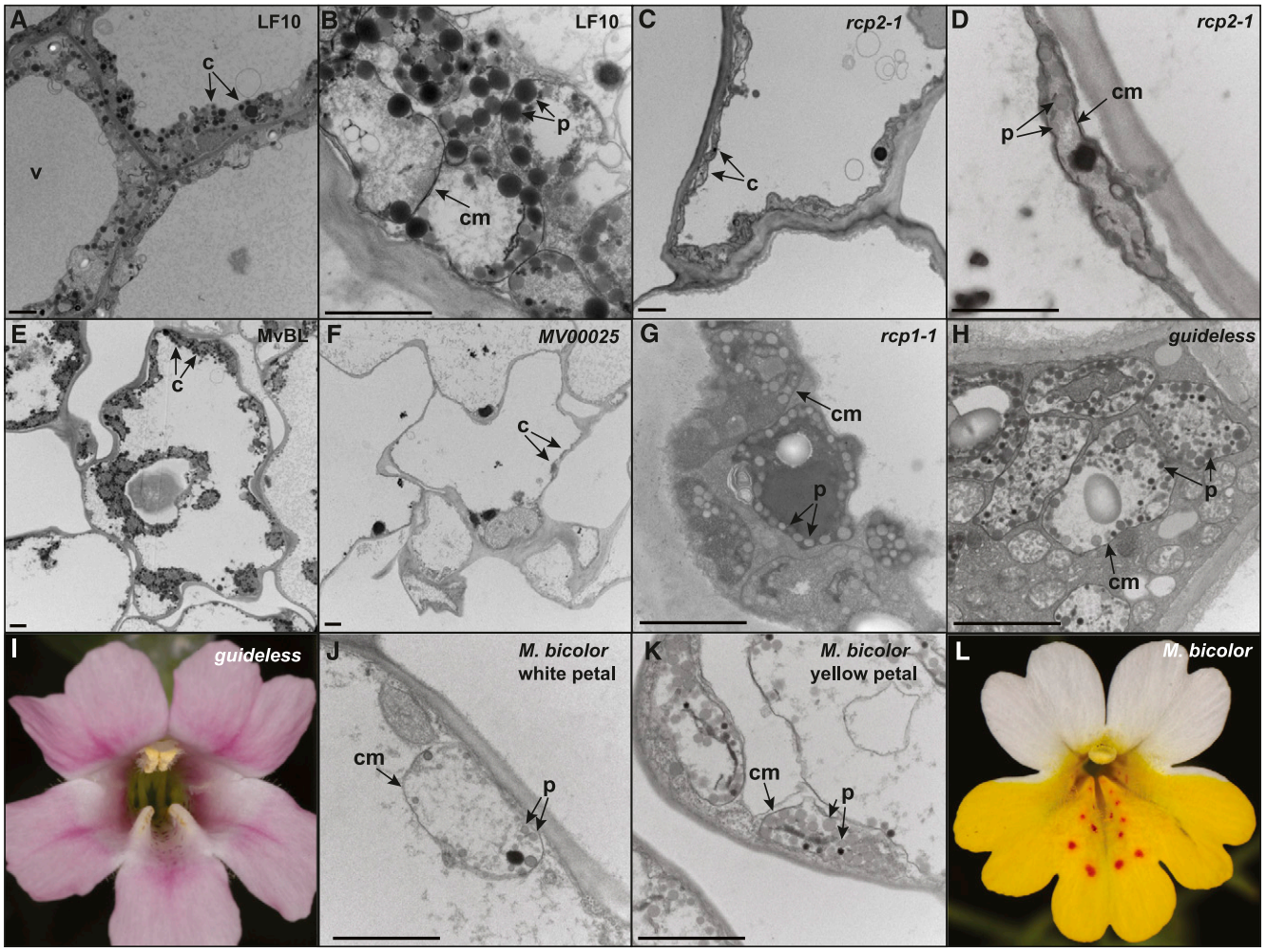

Figure 6. Transmission Electron Micrographs of Chromoplasts.

(A) and **(B)** Micrographs of *M. lewisii* wild-type LF10 nectar guide upper epidermal cells (section from the center of the nectar guide): whole-cell view **(A)** and detailed view of chromoplasts **(B)**.

(C) and **(D)** Micrographs of *M. lewisii rcp2-1* mutant nectar guide upper epidermal cells, sampled and presented in the same fashion as in **(A)** and **(B)**, respectively.

(E) and **(F)** Whole-cell view of petal lobe upper epidermal cells of *M. verbenaceus* wild-type MvBL **(C)** and *MV00025* **(D)**.

(G) and **(H)** Detailed view of chromoplasts from nectar guide upper epidermal cells of the *M. lewisii* mutants *rcp1-1* **(G)** and *guideless* **(H)**.

(I) Front view of *M. lewisii guideless* flower.

(J) and **(K)** Detailed view of plastids from the upper epidermis of the white dorsal petal **(J)** and the yellow ventral petal **(K)** of *M. bicolor.*

(L) Front view of *M. bicolor* flower. v, Vacuole; c, chromoplast; P, plastoglobule; cm, chromoplast membrane. Scale bars are 2 μm.

both *rcp1-1* and another mutant with greatly reduced carotenoid pigmentation in the nectar guides, *guideless* (Figure 6I; Yuan et al. 2013a), should also exhibit abnormal chromoplast development. However, in these mutants, chromoplasts appear normal in shape (Figures 6G and 6H), unlike the skinny, abnormally shaped chromoplasts in *rcp2* petals. The plastoglobuli are smaller and less electron-dense in *rcp1* and *guideless* than in the wild type, as one would expect if carotenoids are less abundant. Furthermore, we compared the plastids in the completely white upper petals of another *Mimulus* species, *Mimulus bicolor*, to its yellow lower petals (Figures 6J to 6L). We found that the white petals, though lacking carotenoids, make plastids similar in appearance to the chromoplasts made in the yellow petals of the same flower. These observations suggest that the defective chromoplast development in *rcp2* mutants is not due to the lack of carotenoid pigments per se but is a more direct consequence of *RCP2* malfunction.

RCP2 Regulates Carotenoid Biosynthesis Independently of *RCP1*

To test potential genetic interactions between *RCP1* and *RCP2*, we created the *rcp1-1 rcp2-1* double mutant. The double mutant shows an additive phenotype regarding the spatial distribution of residual carotenoids, which are completely absent at both the base (as in *rcp2-1*) and the throat (as in *rcp1-1*) of the corolla tube (Figure 7A). The additive phenotype suggests that *RCP1* and *RCP2* most likely act independently in the regulation of carotenoid biosynthesis. Consistent with this inference, neither of these genes regulates the other at the transcriptional level. qRT-PCR assays showed no significant difference in the transcript level of *RCP2* between the *rcp1-1* mutant and the wild type. Likewise, *RCP1* transcript level did not differ between the *rcp2-1* mutant and the wild type (Figure 7B). In addition, a yeast two-hybrid assay showed no direct interaction between the RCP1 and RCP2 proteins (Supplemental Figure 3). Furthermore, *RCP1* and *RCP2* have very different spatiotemporal expression patterns: while *RCP1* expression is restricted to the nectar guides (Sagawa et al., 2016) and peaks at the 10-mm corolla developmental stage, *RCP2* is expressed in both nectar guides and petal lobes and gets stronger over the course of flower development (Figure 5C).

RCP2 Overexpression Promotes Ectopic Carotenoid Biosynthesis and Potentially Chromoplast Proliferation

To further characterize the function of *RCP2*, we generated transgenic plants overexpressing this gene. Because the dominant *YUP* allele represses carotenoid accumulation in the *M. lewisii* flower (except the nectar guides; Hiesey et al. 1971), we performed the overexpression experiment in *M. verbenaceus*, which is homozygous for the recessive *yup* allele. We transformed MvBL with a *35S:RCP2-yellow fluorescent protein* (*YFP*) construct and obtained seven stable transgenic lines, five of which showed a similar overexpression phenotype, with increased carotenoid contents in the flower, particularly the style and filaments (Figures 8A, 8B, and 8I). Correspondingly, the expression levels of CBP genes increased substantially in these tissues (Figures 8A and 8B; Supplemental Figure 4). Cells at the upper, middle, and the lower portions of both style and filaments appear to have not only yellower, but potentially more numerous chromoplasts in the *35S:RCP2-YFP* plants than in the wild type (Figures 8C to 8H). Because the exact number of chromoplasts per cell is difficult to quantify, we assayed relative expression levels of the plastid division genes *MvFtsZ1*, *MvFtsZ2*, *MvARC1*, and *MvARC6* in developing flower buds as a proxy. We found that *MvARC1* and *MvARC6* were slightly, but significantly, up-regulated (~1.5-fold) in the overexpression plants (Figure 8J). Although the function of these plastid division genes in chloroplast division has been well characterized (Osteryoung and Pyke, 2014), their role in chromoplast division is still largely hypothetical. As such, we can only tentatively conclude that *RCP2* overexpression promotes chromoplast proliferation in filaments and styles.

It should be noted that *RCP2* overexpression does not appear to cause carotenoid accumulation in colorless plastids in the roots (i.e., amyloplasts; Supplemental Figure 5), indicating that not all tissue types are competent to produce carotenoids upon *RCP2* expression.

Subcellular Localization of RCP2 Does Not Change upon Amitrole Treatment

To gain insight into the functional mechanism of RCP2, we attempted to determine the subcellular localization of the protein

Figure 7. Lack of Genetic Interaction between *RCP1* and *RCP2*.

(A) Front view and nectar guide view of the *rcp1-1 rcp2-1* double mutant. White and red boxes indicate the base and throat of the corolla tube, respectively.
(B) qRT-PCR experiments showing the relative expression of *RCP2* in the 15-mm nectar guides of the *rcp1* mutant compared to the wild type and *RCP1* in the 10-mm nectar guides of the *rcp2* mutant compared to the wild type. Error bars are 1 SD ($n = 3$ biological replicates, each consisting of pooled 15 [for *RCP2*]- or 10-mm (for *RCP1*) nectar guides from a distinct plant; NS, non-significant; Student's *t* test).

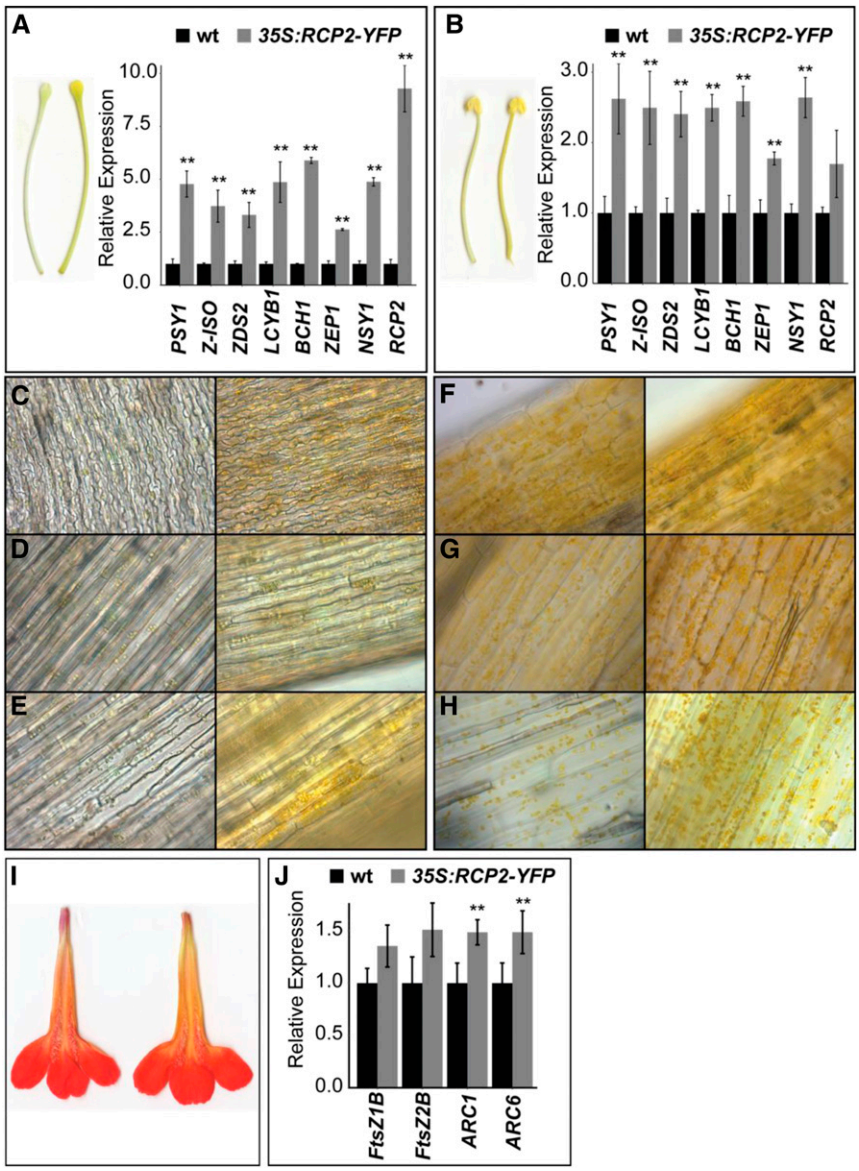

Figure 8. Overexpression of *RCP2* in *M. verbenaceus*.

(A) The phenotypes of wild-type (left) and *35S:RCP2-YFP* (right) styles, and the relative transcript levels of *RCP2* and a subset of CBP genes in the style tissue of 15-mm corollas. Error bars are 1 SD ($n = 3$ biological replicates, each consisting of pooled 15-mm stage styles from a distinct T2 plant of transgenic line 6).
(B) Filament phenotypes and relative gene expression levels shown in the same fashion as in **(A)**.
(**C**) to **(E)** Light microscopy of wild-type (left) and *35S:RCP2-YFP* (right) styles, showing the top **(C)**, middle **(D)**, and base **(E)** of the style.
(**F**) to **(H)** Light microscopy of filaments, shown in the same manner as in **(C)** to **(E)**.
(I) The lower petals of wild-type (left) and *35S:RCP2-YFP* (right) corollas.
(J) Relative expression of the plastid division genes in the 2-mm flower buds of *35S:RCP2-YFP* compared to wild-type plants. Error bars are 1 SD ($n = 3$ biological replicates, each consisting of pooled 2-mm flower buds from a distinct T2 plant of transgenic line 6). Asterisks indicate differences from the wild type (**$P < 0.01$, Student's *t* test).

using the *35S:RCP2-YFP* plants. Unexpectedly, no fluorescence was observed, which was surprising because (1) the same YFP tag fused to the C termini of other proteins have been previously shown to emit strong fluorescence in *Mimulus* (Ding and Yuan, 2016); (2) the chimeric RCP2-YFP protein was clearly functional, as it produced overexpression phenotypes in the wild-type background (Figure 8) and resulted in phenotypic rescue when the *35S:RCP2-YFP* transgene was crossed into the *rcp2* mutant background (Supplemental Figure 4); and (3) REC1-YFP (chimeric protein of the Arabidopsis ortholog of RCP2-L2) showed fluorescence signal in a transient assay in *Nicotiana benthamiana* (Larkin et al., 2016). We therefore performed a transient assay by

agroinfiltrating the *35S:RCP2-YFP* plasmid into *N. benthamiana* leaves, using *35S:RCP1-YFP* as a positive control. While the RCP1-YFP was nuclear localized in *N. benthamiana* pavement cells (Figure 9A), RCP2-YFP still produced no detectable fluorescence signal. We therefore constructed a second overexpression plasmid (*35S:YFP-RCP2*) with the YFP tag fused to the N terminus of RCP2 and tested its localization in *N. benthamiana* leaves. This experiment showed cytonuclear localization (Figure 9B; Supplemental Figure 3), which is consistent with that of REC1-YFP (Larkin et al., 2016).

Larkin et al. (2016) showed that the blockage of carotenoid and chlorophyll biosynthesis by amitrole treatment in *N. benthamiana* leaves caused REC1 to be excluded from the nucleus. To test whether RCP2 has the same behavior, we treated *N. benthamiana* plants with 125 μM amitrole solution and performed transient assays using the *35S:YFP-RCP2* construct. The white leaves of amitrole-treated plants showed no change in protein localization compared to the leaves of mock-treated plants: fluorescence was still localized to both the nucleus and cytosol (Figure 9C). These results differ from those of Arabidopsis REC1 (Larkin et al., 2016), indicating functional divergence of these proteins.

RCP2-like Genes Affect Chlorophyll Accumulation and Chloroplast Coverage in Leaves

The *RCP2* homologs in Arabidopsis (*REC1*/*REC2*/*REC3*) regulate chlorophyll accumulation and the chloroplast compartment size in leaf mesophyll cells. Some of the Arabidopsis combinatorial mutants show clear chlorophyll deficiency (Larkin et al., 2016).

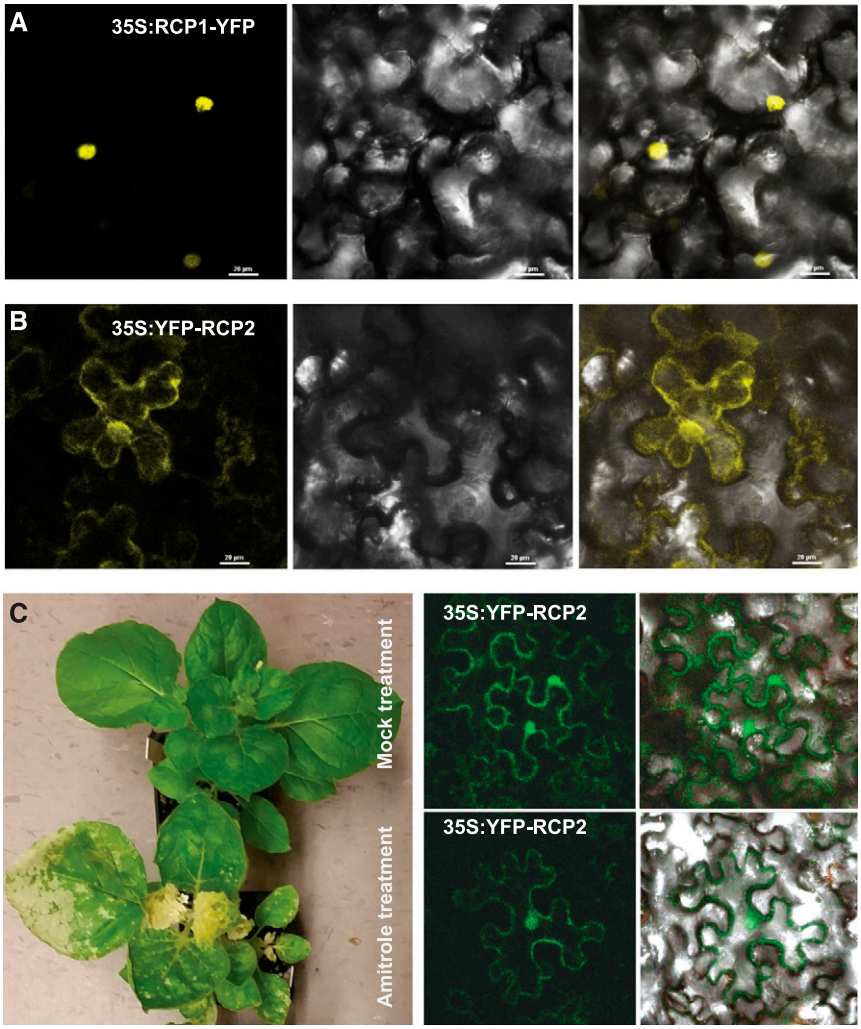

Figure 9. Protein Localization in *Nicotiana benthamiana*.

(A) and **(B)** Confocal microscopy of leaves transiently infiltrated with the plasmid *35S:RCP1-YFP* **(A)** and *35S:YFP-RCP2* **(B)**. Left, Green channel; middle, transmitted light; right, merged. Scale bars are 20 μm.

(C) RCP2 localization does not change after amitrole treatment (bottom) compared to mock-treated plants (top). For each transient assay, five patches of ~50 cells near injection sites were examined. Localization patterns were all the same as those shown in the figure.

rcp2 mutants in both *M. lewisii* (not shown) and *M. verbenaceus* have leaves similar in appearance to wild-type plants (Figure 10A). Pigment extractions from *M. verbenaceus* leaves showed that the chlorophyll content of the mutant *MV00025* is not significantly different from that of the wild type (Figure 10B). However, carotenoid content is slightly lower in *MV00025* than the wild type (Figure 10C).

If the function of *RCP2*-like genes in the regulation of chlorophyll accumulation and chloroplast compartment size is conserved between Arabidopsis and *Mimulus*, we expect that disrupting the function of *RCP2*, *RCP2-L1*, and *RCP2-L2* simultaneously would cause chlorophyll deficiency in photosynthetic tissues. To test this hypothesis, we attempted to induce a dominant-negative effect by overexpressing only the TPR domain of RCP2. The rationale is that

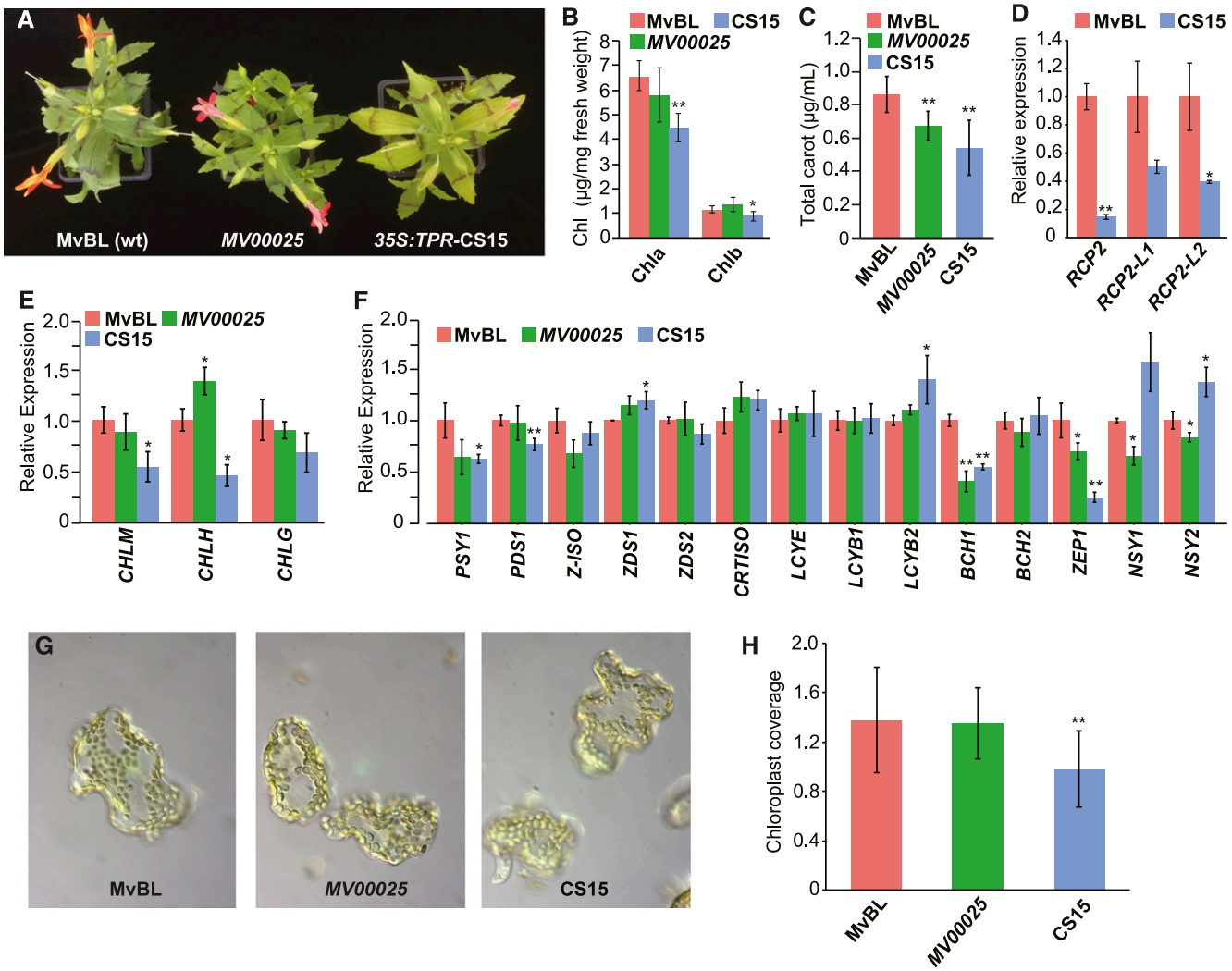

Figure 10. Phenotypic Effects of Simultaneous Down-Regulation of *RCP2*, *RCP2-L1*, and *RCP2-L2* in *Mimulus verbenaceus*.

(A) Left to right, wild-type (MvBL), *rcp2* mutant, and *35S:TPR* cosuppression line 15.
(B) Chlorophyll a and b concentrations in the distal half of 30-mm leaves. Error bars are 1 SD ($n = 6$ different leaves from the same plant).
(C) Total carotenoid content of the distal half of leaves, calculated by measuring carotenoid absorption at 470 nm and subtracting the concentrations of chlorophylls a and b. Error bars are 1 SD ($n = 10$ different leaves from the same plant).
(D) Relative transcript levels of *RCP2*, *RCP2-L1*, and *RCP2-L2* in 10-mm leaves of cosuppression line 15 (CS15) compared to the wild type. Error bars represent 1 SD ($n = 3$ biological replicates, each consisting of pooled 10-mm leaves from a distinct T2 plant of cosuppression line 15).
(E) and **(F)** Relative transcript levels of chlorophyll **(E)** and carotenoid **(F)** biosynthesis genes in 10-mm leaves of the *rcp2* mutant and cosuppression plants compared to the wild type. Error bars represent 1 SD ($n = 3$ biological replicates, each consisting of pooled 10-mm leaves from a distinct MvBL, *MV00025*, or T2 plant of cosuppression line 15).
(G) Representative mesophyll cells of 30-mm leaves from the wild type, *rcp2* mutant, and cosuppression plants.
(H) Chloroplast coverage in MvBL, *MV00025*, and CS15 mesophyll cells. Error bars are 1 SD ($n = 18$ cells for MvBL, $n = 17$ cells for *MV00025* and $n = 13$ cells for CS15). Asterisks indicate differences from the wild type (*$P < 0.05$, **$P < 0.01$, Student's *t* test).

the TPR domain is known to mediate protein-protein interactions, and overexpression of the TPR domain alone has been demonstrated to phenocopy loss-of-function mutations in other TPR genes (Chen et al., 1996; Tseng et al. 2001). Assuming that RCP2, RCP2-L1, and RCP2-L2 function redundantly in photosynthetic tissues by interacting with the same partners, overexpression of the RCP2 TPR domain should interfere with the function of all three proteins. To this end, we transformed wild-type *M. verbenaceus* (MvBL) with a *35S:TPR* construct and generated 36 stable transgenic lines. Somewhat surprisingly, only four of the 36 lines have a pale-leaf phenotype (Figure 10A) resembling the combinatorial *rec* mutants in Arabidopsis, as one would expect from a dominant-negative effect. The flowers of these four lines are also completely pink without carotenoids. Upon further examination, we determined that these phenotypes are actually caused by cosuppression rather than a dominant-negative effect, as all three genes are down-regulated at the transcript level (Figure 10D). The DNA sequence encoding the RCP2 TPR domain has ~80% identity to that of *RCP2-L1/L2*, which explains the relatively weak down-regulation of these two genes (~50% knock-down) compared with *RCP2* itself (~85% knock-down).

Both chlorophyll and carotenoid contents in the leaf are significantly reduced in the cosuppression plants compared with wild type (Figures 10B and 10C), although the relative compositions of individual chlorophyll or carotenoid species show no obvious differences (Supplemental Figure 6; Supplemental Table 1). Correspondingly, the chlorophyll biosynthesis genes *CHLM* and *CHLH* (but not *CHLG*) are modestly but significantly down-regulated (~50%) in the leaves of cosuppression plants but not in the *rcp2* mutant (*MV00025*; Figure 10E). These results indicate that either *RCP2* is not involved, or its function is redundant with that of *RCP2*-like genes, in the regulation of chlorophyll biosynthesis. The expression changes of CBP genes in the leaf, on the other hand, are more complex. For instance, *PSY1* and *BCH1* were down-regulated in both the *rcp2* mutant and cosuppression line to a similar degree; *ZEP1* expression showed a ~30% reduction in the *rcp2* mutant, but ~75% reduction in the cosuppression line; both *NSY* paralogs showed slightly lower expression in the *rcp2* mutant but higher expression in the cosuppression line; and several other genes showed no expression change between the wild type and either *rcp2* or the cosuppression plants (Figure 10F).

Similar to the *rec* mutants in Arabidopsis, our cosuppression plants show no obvious differences in chloroplast morphology but have reduced chloroplast compartment size compared with the wild type (Figures 10G and 10H; Supplemental Figure 7). The decrease in chloroplast coverage is less dramatic in our cosuppression plants (~28%) than in some of the combinatorial *rec* mutants (~50%). This is likely because the down-regulation of *RCP2-L1* and *RCP2-L2* was relatively weak in the cosuppression plants (Figure 10D), in contrast to the null alleles of *REC1/2/3* characterized in Arabidopsis (Larkin et al., 2016). This interpretation is also consistent with our observation that chlorophyll content in the cosuppression plants decreased by only ~30% compared with wild-type plants (Figure 10B), whereas *Arabidopsis rec1 rec2 rec3* triple mutants showed ~80% decrease in chlorophyll content. Taken together, these results demonstrate that the function of this small family of TPR genes in regulating chlorophyll accumulation and chloroplast compartment size in photosynthetic tissues is conserved between Arabidopsis and *Mimulus*.

DISCUSSION

In this study, we characterized the *RCP2* locus in *M. lewisii* and its close relative *M. verbenaceus*. Based on genetic mapping, multiple independent mutant alleles, transgenic experiments, and TEM analyses, we demonstrated that *RCP2* encodes a TPR protein that is necessary and sufficient for chromoplast development and CBP gene expression in *Mimulus* floral tissues. We also showed that simultaneous down-regulation of *RCP2* and its two paralogs, *RCP2-L1* and *RCP2-L2*, leads to reduced chlorophyll and carotenoid content as well as chloroplast compartment size in leaves.

RCP2 Positively Regulates Both Chromoplast Development and CBP Gene Expression in *Mimulus* Flowers

Our TEM results (Figure 6) suggest that one of the primary functions of *RCP2* is in the regulation of chromoplast development, independently of carotenoid biosynthesis, as other *Mimulus* flowers with reduced carotenoid accumulation produce petal plastids with the typical rounded shape (Figures 6G to 6L). Gene expression analyses of the *rcp2* mutants and *RCP2* overexpression lines showed that *RCP2* is also a positive regulator of CBP gene expression (Figures 1E, 2D, 8A, and 8B). However, our current data cannot distinguish whether the role of *RCP2* in CBP gene activation is independent of, or secondary to, chromoplast development.

The phenotypic effect of *RCP2* overexpression in *Mimulus* floral tissues is superficially similar to that of the gain-of-function mutations in the cauliflower and melon *Orange* (*Or*) gene and loss-of-function mutations in tomato *High Pigment-1*, *High Pigment-2*, and *High Pigment-3* genes (encoding DDB1, DET1, and ZEP, respectively), in terms of increased carotenoid content and altered chromoplast biogenesis. However, there are key differences. While RCP2 positively regulates the entire CBP at the transcriptional level, OR and HP-1/HP-2/HP-3 do not affect steady-state mRNA levels of CBP genes in general (Li et al., 2001; Cookson et al., 2003; Kolotilin et al., 2007; Galpaz et al., 2008; Yuan et al., 2015). The cauliflower mutant OR allele ($BoOR^{MUT}$) and the melon OR "golden SNP" ($CmOR^{His}$) enhance carotenoid accumulation in nonphotosynthetic tissues by stabilizing the PSY protein, triggering the formation of membranous chromoplasts and inhibiting β-carotene turnover (Lu et al., 2006; Tzuri et al., 2015; Yuan et al., 2015; Zhou et al., 2015; Chayut et al., 2017). Loss-of-function mutations in the *HP* genes produce tomato fruits with increased chlorophyll and carotenoid content due to increased plastid size and/or number (Cookson et al., 2003; Kolotilin et al., 2007; Galpaz et al., 2008), with no effect on CBP gene transcription. These differences suggest that *RCP2* has a distinct function from these previously characterized genes involved in plastid development and carotenoid regulation.

The biochemical functions of RCP2 and RCP2-like proteins are still poorly understood. Larkin et al. (2016) conducted an extensive genetic characterization of all four members of this small TPR gene family in Arabidopsis (i.e., *REC1/2/3* and *FRIENDLY*). They demonstrated that the REC1 protein (ortholog of RCP2-L2;

Figure 4) localizes to both the cytosol and the nucleus but is excluded from the nucleus upon amitrole treatment, which blocks chloroplast biogenesis. They suggested that this trafficking of REC1 between the nucleus and the cytosol might be important for the function of REC1 in maintaining a proper chloroplast compartment size. Beyond protein localization, very little information is available about the functional mechanisms of this small family of TPR proteins. Given that the TPR repeats are well known to serve as scaffolds mediating protein-protein interactions (D'Andrea and Regan, 2003; Zeytuni and Zarivach, 2012; Bohne et al., 2016), identifying the putative interacting partners of RCP2 and RCP2-like proteins may help elucidate their functional mechanisms in regulating plastid development and pigment biosynthesis.

Although carotenoid content decreased in the leaves of our cosuppression plants compared to the wild type (Figure 10C), there is no clear pattern of wholesale CBP gene down-regulation (Figure 10F), as observed in the flowers. These results indicate that the regulation of carotenoid accumulation in leaf tissue is more complex than in floral tissue, likely involving regulators in addition to *RCP2* or *RCP2*-like genes. This is not surprising, given that carotenoids in leaves are essential components of the photosynthetic apparatus (Liu et al., 2004b; Amunts et al., 2010), and their content and composition are tightly coregulated with other components of photosynthesis by both transcriptional and posttranslational mechanisms (Meier et al., 2011; Ruiz-Sola and Rodríguez-Concepción, 2012; Nisar et al., 2015; Sun and Li, 2020). By contrast, in flower petals, carotenoids are stored in chromoplasts as dispensable, secondary metabolites, and the regulation of carotenoid accumulation is decoupled from photosynthesis.

While the molecular mechanism of RCP2 remains to be elucidated, the finding that *RCP2* overexpression can increase both the biosynthetic activity and storage capacity of carotenoids, through coordinated CBP gene up-regulation and chromoplast development, respectively (Figure 8), suggests that *RCP2* represents an attractive target for carotenoid biofortification in crops.

Functional Conservation and Divergence of the *REC*/*RCP2* Gene Family Members

Our phylogenetic analysis shows that the *REC*/*RCP2*-like TPR genes in angiosperms fall into three well-supported clades (i.e., *REC1*/*RCP2-L2*, *REC2*/*RCP2*, and *REC3*/*RCP2-L1*; Figure 4), which is consistent with the results reported in Larkin et al. (2016). The three paralogs had already evolved in the common ancestor of all angiosperms. While the closely related *FRIENDLY* gene has a highly conserved function in regulating the intracellular distribution of mitochondria in a wide range of eukaryotes (Zhu et al., 1997; Fields et al., 1998; Logan et al., 2003; Cox and Spradling, 2009; Gao et al., 2014), whether the *REC* genes have a conserved role in regulating chlorophyll biosynthesis and chloroplast compartment size has been unclear. The simultaneous down-regulation of *RCP2*, *RCP2-L1*, and *RCP2-L2* in our cosuppression plants resulted in significant decrease in chlorophyll content and chloroplast compartment size (Figures 10B and 10H), suggesting that the role of these TPR genes in regulating chlorophyll accumulation and chloroplast compartment size is conserved between Arabidopsis and *Mimulus*.

The existence of three paralogs provides opportunities for functional divergence. For example, while the *Arabidopsis rec1* mutant is a *genomes uncoupled* (*gun*) mutant with disrupted chloroplast-to-nucleus signaling, *rec2* and *rec3* appear to have intact retrograde signaling (Larkin et al., 2016). Arabidopsis REC1 shows altered protein localization upon amitrole treatment (i.e., from cytonuclear to exclusively cytoplasmic), but the REC2 ortholog in *Mimulus*, RCP2, does not seem to have this behavior (Figure 9C). Furthermore, the FRIENDLY protein is exclusively localized to the cytosol in wild-type Arabidopsis (Logan et al., 2003; El Zawily et al., 2014), indicating that this nucleus-to-cytosol trafficking behavior might be specific to REC1 (and potentially its orthologs in other plants).

In addition to protein function, the expression patterns of these three genes have also diverged. In *Mimulus*, while *RCP2-L1* and *RCP2-L2* are primarily expressed in photosynthetic tissues, *RCP2* is expressed only weakly in leaves (and is not expressed in stems). Instead, this gene is strongly expressed in the corolla throughout flower development (Figure 5A). The evolution of the diverged *RCP2* paralog may allow for pigment/plastid innovation in non-green tissues such as flowers, while the *RCP2*-like genes continue to perform essential functions in photosynthetic tissues. *RCP2* and its orthologs in other species may therefore have great potential for generating natural variation in floral carotenoid pigmentation.

Mimulus verbenaceus Is an Excellent Developmental Genetics Model System Complementary to *M. lewisii*

Our results also demonstrate that the hummingbird-pollinated *M. verbenaceus* is just as amenable to chemical mutagenesis and in planta transformation as the more extensively studied, bumblebee-pollinated *M. lewisii*. This is significant because *M. verbenaceus* provides an excellent study system complementary to *M. lewisii*, allowing us to carry out experiments that might be challenging to interpret in *M. lewisii*. For example, *RCP2* overexpression produces clear phenotypes in *M. verbenaceus* floral tissues that might otherwise be masked in *M. lewisii* by the dominant *YUP* allele (Hiesey et al., 1971). In addition, despite being genetically very similar (Beardsley et al., 2003), these two species differ drastically in terms of many pollinator-associated floral traits. Given the ease of chemical mutagenesis in *M. verbenaceus* (e.g., recovery of more than 100 floral mutants from 460 M2 families), it is not difficult to envision that *M. verbenaceus* could become a key model system to dissect the genetic networks underpinning the evolution of hummingbird pollination syndromes (e.g., long stamen and pistil length, copious nectar production). Together, these two species provide an excellent platform for comparative developmental genetics studies of two closely related species with dramatic phenotypic divergence.

METHODS

Plant Materials

The *Mimulus lewisii* Pursh inbred line LF10 (wild type) and the mapping line SL9 were described in Yuan et al. (2013a, 2013b). Seeds of wild *Mimulus verbenaceus* were collected from Oak Creek Canyon (Sedona, Arizona)

and the inbred line MvBL was generated by single seed descent for >10 generations. EMS mutants were generated using LF10 and MvBL for *M. lewisii* and *M. verbenaceus*, respectively, following Owen and Bradshaw (2011). All plants were grown with FAFARD soil mix no. 2 (Sun Gro Horticulture) in the University of Connecticut EEB Research Greenhouses, under natural light either supplemented with sodium vapor lamps or shaded with greenhouse curtain systems, to provide a 16 h daylength with a light intensity of 110 to 160 $\mu mol \cdot m^{-2} \cdot s^{-1}$. Plants were watered by subirrigation and fertilized three times a week.

Carotenoid and Chlorophyll Analyses

To estimate relative carotenoid concentration in *M. lewisii* corollas, carotenoid pigments were extracted from the nectar guides of fresh flowers as described in Sagawa et al. (2016). Carotenoid concentration was estimated based on absorbance measurement at 440 nm and normalized to 100 mg tissue.

To determine chlorophyll concentration in *M. verbenaceus* leaf tissue, carotenoids and chlorophylls were extracted together from the distal half of 30-mm leaves in 1 mL methanol. Chlorophyll concentration was estimated using the following equations (Lichtenthaler, 1987):

$$[Chlorophyll\ a\ ] = 16.72 \times A665 - 9.16 \times A652$$

$$[Chlorophyll\ b\ ] = 34.09 \times A652 - 15.28 \times A665$$

The relative carotenoid concentration and composition in *M. verbenaceus* leaves were determined using ultraviolet–visible spectroscopy and high-performance liquid chromatography (HPLC). Leaves were collected from wild-type MvBL, *MV00025*, and CS15 plants, and tissue weighing 30 mg was trimmed from the distal tip of each leaf. Pigments were extracted by grinding tissue in 1 mL of methanol, pelleting the leaf tissue by centrifugation, and isolating the supernatant. Absorption spectra of extracts from 10 leaves of each line were measured using a Varian Cary 50 ultraviolet–visible spectrometer. A 200-μL aliquot of each sample was diluted 1:9 (v/v) with fresh methanol and measured in a 1-cm quartz cuvette. Total carotenoid content was calculated (g/mL of total extract) by measuring the carotenoid absorption at 470 nm and subtracting the concentrations of chlorophylls a and b, as described by Lichtenthaler (1987).

HPLC analysis was conducted for two leaves per line using a Waters 600 multisolvent delivery system equipped with a Waters 2996 photodiode array detector and a Waters Atlantis T3 column (5 particle size, 4.6 × 250 mm). A 400-μL aliquot of each sample was diluted with 600 μL of acetonitrile and filtered through a Millipore 0.2 m Millex-FG syringe filter. The mobile phase consisted of solvent A, 87:10:3 (v/v/v) acetonitrile:methanol:water; and solvent B, ethyl acetate. Chromatography was performed using the following gradient: 0 to 20 min, 99% A, 1% B (v/v); 20 to 40 min, linear gradient to 60% A, 40% B; 40 to 60 min, 60% A, 40% B. All solvents were purchased from Fisher Scientific and were HPLC-grade quality. The mobile phase flow rate was 1.2 mL/min, and the injection volume was 200 μL. The percent molar composition of each carotenoid was determined from the chromatograms as described in Lunch et al. (2013).

Separation of Anthocyanins and Carotenoids in *M. verbenaceus* Flowers

The red color of *M. verbenaceus* flowers is due to a combination of high concentrations of carotenoids and anthocyanins. To help visualize the relative carotenoid content in wild-type flowers versus the *rcp2* mutants or transgenic lines, we separated anthocyanins and carotenoids. This was accomplished by grinding two petal lobes in 200 μL methanol, which dissolves both carotenoids and anthocyanins. After 2 min of centrifugation at 13,000 rpm, 150 μL of the clear pigment extract was transferred to a new tube and thoroughly mixed with 150 μL of water and 150 μL of dichloromethane. The pigments were separated by centrifugation (13,000 rpm for 2 min): water-soluble anthocyanins were suspended in the aqueous phase, while hydrophobic carotenoids remained in the organic phase (Figures 2A to 2C and 3F).

Bulk Segregant Analysis

Genetic mapping of *RCP2* followed the protocol laid out in Yuan et al. (2013a). In short, we crossed *rcp2-1* (which was produced in the LF10 background) with the mapping line, SL9, and selfed an F1 individual to produce an F2 population. We extracted DNA from 120 F2 individuals displaying the mutant phenotype and pooled the samples for deep sequencing on an Illumina HiSeq 2500 platform. We mapped the ~196 million reads (Bioproject: PRJNA326848) to the SL9 genome using CLC Genomics Workbench 7.0 (Qiagen) and then scanned for regions enriched in homozygous single nucleotide polymorphisms. This allowed us to identify a 70-kb candidate region.

qRT-PCR

We extracted RNA and synthesized cDNA according to Yuan et al. (2013b). The relative transcript levels of carotenoid biosynthetic genes, chlorophyll biosynthetic genes, plastid division genes, as well as *RCP1* and *RCP2*, were assessed by qRT-PCR (primers are listed in Supplemental Table 2). qRT-PCR was performed using Power SYBR Green PCR master mix (Applied Biosystems) on a CFX96 touch real-time PCR detection system (Bio-Rad). Samples were amplified for 40 cycles of 95°C for 15 s and 60°C for 30 s. Amplification efficiencies for each primer pair were determined using critical threshold values obtained from a dilution series (1:4, 1:8, 1:16, 1:32) of pooled cDNAs. *MlUBC*, the *Mimulus* ortholog of the Arabidopsis ubiquitin-conjugating enzyme gene (AT5G25760), was used as the reference gene as described in Yuan et al. (2013b). Three biological replicates, with a single technical replicate for each sample, were used for all qRT-PCR experiments; see the figure legends for details. Relative expression of each target gene compared to the reference gene was calculated using the formula $(E_{ref})^{CP(ref)}/(E_{target})^{CP(target)}$.

Phylogenetic Analysis

Multiple sequence alignment of RCP2 and related proteins was performed using MUSCLE (Edgar, 2004). Only the three conserved domains (CLU_N, CLU_central, and TPR domain) that could be confidently aligned across all sequences (Supplemental Data Set 2) were used for phylogenetic analysis. Maximum likelihood analysis was conducted using the RAxML web server (https://raxml-ng.vital-it.ch/#/; Kozlov et al., 2019), with the Jones-Taylor-Thornton amino acid substitution matrix and the GAMMA model of rate heterogeneity. Clade support was estimated by 100 bootstrap replicates. The tree (Supplemental Data Set 3) was rooted by midpoint rooting.

RNAi Plasmid Construction

We built an RNAi construct by cloning a 408-bp fragment of exon 23 of the *M. lewisii RCP2* gene into the pFGC5941 vector (Kerschen et al., 2004) in both the sense and antisense directions, following Yuan et al. (2013b; primers are listed in Supplemental Table 3). This fragment, and every 12-bp block within it, matched only a single region of the *M. lewisii* (100% identity) and *M. verbenaceus* genomes (95% identity), indicating target specificity. The plasmid was verified by sequencing and transformed into *Agrobacterium tumefaciens* (strain GV3101), before being transformed into wild-type LF10 and MvBL plants by vacuum infiltration following the protocol described in Yuan et al. (2013b).

Overexpression Constructs and Protein subcellular localization

To characterize the phenotypes caused by overexpression of *RCP2* and to visualize the subcellular localization of RCP2 proteins, the 5382-bp full-length *RCP2* coding DNA sequence (CDS) was cloned into two different Gateway vectors: pEarleyGate 101 and pEarleyGate 104 (Earley et al., 2006), as previously described (Yuan et al., 2014). These vectors drive expression of the transgene by the cauliflower mosaic virus *35S* promoter. In pEarleyGate 101 and pEarleyGate 104, the YFP CDS is fused in frame with the 3′ end and 5′ end of the *RCP2* CDS, respectively (i.e., *35S:RCP2-YFP* and *35S:YFP-RCP2*, respectively). In an attempt to generate a dominant-negative effect by overexpressing only the RCP2 TPR domain, we amplified a 1227-bp fragment of the *RCP2* CDS that encodes the TPR domain and cloned it into pEarleyGate 100 (i.e., *35S:TPR*), the same destination vector as pEarleyGate 101 without the YFP tag. All overexpression plasmids were sequence verified before being transformed into *Agrobacterium tumefaciens* (strain GV3101). The *35S:RCP2-YFP* and *35S:TPR* constructs were transformed into MvBL plants to generate stable transgenic lines.

For transient protein expression, Agrobacterium solutions containing either the *35S:YFP-RCP2* or *35S:RCP2-YFP* plasmid were injected to the abaxial side of *Nicotiana benthamiana* leaves, following Ding and Yuan (2016). Fluorescence images were acquired using a Nikon A1R confocal laser scanning microscope equipped with a 60× water immersion objective. We performed immunoblot analysis to test whether the transiently expressed YFP-RCP2 protein was intact. *N. benthamiana* leaf tissue transfected with the *35S:YFP-RCP2* plasmid was harvested 6 d after inoculation. Total plant protein was extracted using the plant total protein extraction kit (Sigma) according to the manufacturer's instructions. Extracts were boiled in SDS sample buffer and loaded on 10% mini-PROTEAN TGX gels (Bio-Rad), prior to transfer onto polyvinylidene difluoride membranes (Millipore) and immunoblotting with the GFP tag monoclonal antibody (GF28R, Thermo Fisher Scientific) following standard protocols.

Yeast Two-Hybrid Assay

Yeast two-hybrid constructs were built using the Matchmaker Gold yeast two-hybrid system (Clontech). The full-length *RCP2* CDS was recombined into the pGBKT7-BD bait vector using an In-Fusion cloning kit (Clontech) and transformed into the Y2H Gold yeast strain by polyethylene glycol transformation, according to manufacturer's instructions. The *RCP1* CDS was recombined in vivo into the pGADT7-AD prey plasmid in the Y187 yeast strain (primers listed in Supplemental Table 3). Both plasmids were brought together in individual yeast cells by mating between the two yeast strains and screened on DDO, QDO, and QDO/X/A plates to test for protein-protein interactions.

TEM

Pieces of nectar guide tissue of *M. lewisii* or petal lobe tissue of *M. verbenaceus* were prefixed in 2.5% glutaraldehyde and 2.0% paraformaldehyde with 0.05 M Pipes buffer. The samples were postfixed with 1% osmium tetroxide and 0.8% $K_3Fe(CN)_6$ and then dehydrated in ethanol. The samples were embedded in Spurr's resin and sectioned tangentially. The sections were counterstained with 2% aqueous uranyl acetate and 2.5% Sato's lead citrate. The sections were examined and photographed under a Tecnai 12 G2 Spirit BioTWIN transmission electron microscope (FEI) at UConn's Bioscience Electron Microscopy Laboratory.

Mesophyll Cell Microscopy and Chloroplast Coverage

Leaf mesophyll cells of wild-type *M. verbenaceus* (MvBL), the *rcp2* mutant MV00025, and the cosuppression line *35S:TPR-CS15* were isolated following Pyke (2011) to examine chloroplast morphology and compartment size. In brief, 35-mm leaves were cut into strips and fixed in 4% glutaraldehyde. The middle lamella was weakened by heating the leaf tissue at 60°C for 4 h in 0.1 M EDTA. Prior to light microscopy, leaf strips were macerated with forceps to separate cells. To consistently count chloroplasts in leaf cells, light microscopy images were taken at different depths, and manual counts were made by marking all chloroplasts in each image and removing any chloroplasts that appeared in multiple images. The cell plan area and average chloroplast plan area (10 chloroplasts/cell) were determined using ImageJ, and chloroplast coverage was calculated using the following equation: (chloroplast number per cell × mean chloroplast plan area per cell)/mesophyll cell plan area (Pyke, 2011). The chloroplast coverage was determined for 13 to 18 mesophyll cells per genotype.

Root Plastid Microscopy

Seeds of wild-type MvBL and *35S:RCP2-YFP* overexpression plants were sown on wet paper towels in Petri dishes sealed with Parafilm. After 7 d, eight seedlings of each genotype were removed from the dish and whole-mounted in water. Root tips were examined and imaged under a light microscope.

Accession Numbers

Sequence data from this article can be found in the GenBank/EMBL libraries under the following accession numbers: *MlRCP2* (MF616356), *MlRCP2-L1* (MF616357), *MlRCP2-L2* (MF616358), *MvRCP2* (MF616359), *MlFRIENDLY1* (MN422297), and *MlFRIENDLY2* (MN422298). Illumina short read data have been deposited in NCBI SRA (accession number PRJNA326848).

Supplemental Data

Supplemental Figure 1. Additional characterization of the *M. lewisii rcp2* and *rcp1* mutants.

Supplemental Figure 2. Alignment of RCP2 and RCP2-like proteins in *M. lewisii* and their homologues in Arabidopsis and *Brachypodium*.

Supplemental Figure 3. Further characterization of the RCP2 protein.

Supplemental Figure 4. Characterization of additional *35S:RCP2-YFP* transgenic plants.

Supplemental Figure 5. Light micrographs of root plastids.

Supplemental Figure 6. HPLC analysis of *M. verbenaceus* leaf pigment composition.

Supplemental Figure 7. Correlations of cell plan area with chloroplast number and plan area.

Supplemental Table 1. Mole percentages of carotenoids in *M. verbenaceus* leaves.

Supplemental Table 2. qRT-PCR primers.

Supplemental Table 3. Primers used for plasmid construction.

Supplemental Data Set 1. Summary of statistical tests.

Supplemental Data Set 2. Sequence alignments for phylogenetic analysis.

Supplemental Data Set 3. Phylogenetic tree file.

ACKNOWLEDGMENTS

We thank Clinton Morse, Matt Opel, and Adam Histen for plant care in the UConn EEB Research Greenhouses, Maritza Abril and Xuanhao Sun at the

UConn Bioscience Electron Microscopy Laboratory for assistance in the TEM experiments, Amy LaFountain (University of Connecticut) for performing the HPLC analysis, and Yuan Gao (Boston University) for assistance in the immunoblot experiment. We thank the editor and three anonymous reviewers for their constructive criticism, which greatly improved the article. This work was supported by the National Science Foundation (grants IOS-1558083 and IOS-1827645 to Y.-W.Y.)

AUTHOR CONTRIBUTIONS

L.E.S. and Y.-W.Y. designed the research; L.E.S., B.D., F.M., C.H., and Y.-W.Y. performed the experiments; W.S. and S.C. contributed Illumina sequencing data; all authors analyzed the data; L.E.S. and Y.-W.Y. drafted the article.

Received September 27, 2019; revised February 3, 2020; accepted February 26, 2020; published March 4, 2020.

REFERENCES

Albert, N.W., Lewis, D.H., Zhang, H., Schwinn, K.E., Jameson, P.E., and Davies, K.M. (2011). Members of an R2R3-MYB transcription factor family in Petunia are developmentally and environmentally regulated to control complex floral and vegetative pigmentation patterning. Plant J. **65:** 771–784.

Ampomah-Dwamena, C., Thrimawithana, A.H., Dejnoprat, S., Lewis, D., Espley, R.V., and Allan, A.C. (2019). A kiwifruit (*Actinidia deliciosa*) R2R3-MYB transcription factor modulates chlorophyll and carotenoid accumulation. New Phytol. **221:** 309–325.

Amunts, A., Toporik, H., Borovikova, A., and Nelson, N. (2010). Structure determination and improved model of plant photosystem I. J. Biol. Chem. **285:** 3478–3486.

Barker, W., Nesom, G., Beardsley, P.M., and Fraga, N.S. (2012). A taxonomic conspectus of Phrymaceae: A narrowed circumscription for *Mimulus*, new and resurrected genera, and new names and combinations. Phytoneuron **39:** 1–60.

Beardsley, P.M., Yen, A., and Olmstead, R.G. (2003). AFLP phylogeny of *Mimulus* section *Erythranthe* and the evolution of hummingbird pollination. Evolution **57:** 1397–1410.

Bemer, M., Karlova, R., Ballester, A.R., Tikunov, Y.M., Bovy, A.G., Wolters-Arts, M., Rossetto, P., Angenent, G.C., and de Maagd, R.A. (2012). The tomato FRUITFULL homologs TDR4/FUL1 and MBP7/FUL2 regulate ethylene-independent aspects of fruit ripening. Plant Cell **24:** 4437–4451.

Bohne, A.-V., Schwenkert, S., Grimm, B., and Nickelsen, J. (2016). Roles of tetratricopeptide repeat proteins in biogenesis of the photosynthetic apparatus. Int. Rev. Cell Mol. Biol. **324:** 187–227.

Borevitz, J.O., Xia, Y., Blount, J., Dixon, R.A., and Lamb, C. (2000). Activation tagging identifies a conserved MYB regulator of phenylpropanoid biosynthesis. Plant Cell **12:** 2383–2394.

Cazzonelli, C.I., Cuttriss, A.J., Cossetto, S.B., Pye, W., Crisp, P., Whelan, J., Finnegan, E.J., Turnbull, C., and Pogson, B.J. (2009). Regulation of carotenoid composition and shoot branching in *Arabidopsis* by a chromatin modifying histone methyltransferase, SDG8. Plant Cell **21:** 39–53.

Chayut, N., et al. (2017). Distinct mechanisms of the ORANGE protein in controlling carotenoid flux. Plant Physiol. **173:** 376–389.

Chen, M.S., Silverstein, A.M., Pratt, W.B., and Chinkers, M. (1996). The tetratricopeptide repeat domain of protein phosphatase 5 mediates binding to glucocorticoid receptor heterocomplexes and acts as a dominant negative mutant. J. Biol. Chem. **271:** 32315–32320.

Chiou, C.-Y., Pan, H.-A., Chuang, Y.-N., and Yeh, K.-W. (2010). Differential expression of carotenoid-related genes determines diversified carotenoid coloration in floral tissues of *Oncidium* cultivars. Planta **232:** 937–948.

Chung, M.Y., Vrebalov, J., Alba, R., Lee, J., McQuinn, R., Chung, J.D., Klein, P., and Giovannoni, J. (2010). A tomato (*Solanum lycopersicum*) APETALA2/ERF gene, SlAP2a, is a negative regulator of fruit ripening. Plant J. **64:** 936–947.

Cookson, P.J., Kiano, J.W., Shipton, C.A., Fraser, P.D., Romer, S., Schuch, W., Bramley, P.M., and Pyke, K.A. (2003). Increases in cell elongation, plastid compartment size and phytoene synthase activity underlie the phenotype of the *high pigment-1* mutant of tomato. Planta **217:** 896–903.

Cox, R.T., and Spradling, A.C. (2009). *Clueless*, a conserved *Drosophila* gene required for mitochondrial subcellular localization, interacts genetically with *parkin*. Dis. Model. Mech. **2:** 490–499.

D'Andrea, L.D., and Regan, L. (2003). TPR proteins: The versatile helix. Trends Biochem. Sci. **28:** 655–662.

Davies, K.M., Albert, N.W., and Schwinn, K.E. (2012). From landing lights to mimicry: The molecular regulation of flower colouration and mechanisms for pigmentation patterning. Funct. Plant Biol. **39:** 619–638.

de Vetten, N., Quattrocchio, F., Mol, J., and Koes, R. (1997). The *an11* locus controlling flower pigmentation in petunia encodes a novel WD-repeat protein conserved in yeast, plants, and animals. Genes Dev. **11:** 1422–1434.

Ding, B., and Yuan, Y.-W. (2016). Testing the utility of fluorescent proteins in *Mimulus lewisii* by an Agrobacterium-mediated transient assay. Plant Cell Rep. **35:** 771–777.

Dong, T., Hu, Z., Deng, L., Wang, Y., Zhu, M., Zhang, J., and Chen, G. (2013). A tomato MADS-box transcription factor, SlMADS1, acts as a negative regulator of fruit ripening. Plant Physiol. **163:** 1026–1036.

Earley, K.W., Haag, J.R., Pontes, O., Opper, K., Juehne, T., Song, K., and Pikaard, C.S. (2006). Gateway-compatible vectors for plant functional genomics and proteomics. Plant J. **45:** 616–629.

Edgar, R.C. (2004). MUSCLE: Multiple sequence alignment with high accuracy and high throughput. Nucleic Acids Res. **32:** 1792–1797.

Egea, I., Barsan, C., Bian, W., Purgatto, E., Latché, A., Chervin, C., Bouzayen, M., and Pech, J.-C. (2010). Chromoplast differentiation: current status and perspectives. Plant Cell Physiol. **51:** 1601–1611.

El Zawily, A.M., et al. (2014). FRIENDLY regulates mitochondrial distribution, fusion, and quality control in *Arabidopsis*. Plant Physiol. **166:** 808–828.

Fields, S.D., Conrad, M.N., and Clarke, M. (1998). The *S. cerevisiae CLU1* and *D. discoideum cluA* genes are functional homologues that influence mitochondrial morphology and distribution. J. Cell Sci. **111:** 1717–1727.

Fu, C.C., Han, Y.C., Fan, Z.Q., Chen, J.Y., Chen, W.X., Lu, W.J., and Kuang, J.F. (2016). The papaya transcription factor CpNAC1 modulates carotenoid biosynthesis through activating phytoene desaturase genes *CpPDS2/4* during fruit ripening. J. Agric. Food Chem. **64:** 5454–5463.

Fu, C.C., Han, Y.C., Kuang, J.F., Chen, J.Y., and Lu, W.J. (2017). Papaya CpEIN3a and CpNAC2 co-operatively regulate carotenoid biosynthesis-related genes *CpPDS2/4, CpLCY-e* and *CpCHY-b* during fruit ripening. Plant Cell Physiol. **58:** 2155–2165.

Fujisawa, M., Nakano, T., and Ito, Y. (2011). Identification of potential target genes for the tomato fruit-ripening regulator RIN by chromatin immunoprecipitation. BMC Plant Biol. **11:** 26.

Fujisawa, M., Nakano, T., Shima, Y., and Ito, Y. (2013). A large-scale identification of direct targets of the tomato MADS box transcription factor RIPENING INHIBITOR reveals the regulation of fruit ripening. Plant Cell **25:** 371–386.

Fujisawa, M., Shima, Y., Higuchi, N., Nakano, T., Koyama, Y., Kasumi, T., and Ito, Y. (2012). Direct targets of the tomato-ripening regulator RIN identified by transcriptome and chromatin immunoprecipitation analyses. Planta **235:** 1107–1122.

Fujisawa, M., Shima, Y., Nakagawa, H., Kitagawa, M., Kimbara, J., Nakano, T., Kasumi, T., and Ito, Y. (2014). Transcriptional regulation of fruit ripening by tomato FRUITFULL homologs and associated MADS box proteins. Plant Cell **26:** 89–101.

Galpaz, N., Wang, Q., Menda, N., Zamir, D., and Hirschberg, J. (2008). Abscisic acid deficiency in the tomato mutant *high-pigment 3* leading to increased plastid number and higher fruit lycopene content. Plant J. **53:** 717–730.

Gao, J., Schatton, D., Martinelli, P., Hansen, H., Pla-Martin, D., Barth, E., Becker, C., Altmueller, J., Frommolt, P., Sardiello, M., and Rugarli, E.I. (2014). CLUH regulates mitochondrial biogenesis by binding mRNAs of nuclear-encoded mitochondrial proteins. J. Cell Biol. **207:** 213–223.

Giménez, E., Pineda, B., Capel, J., Antón, M.T., Atarés, A., Pérez-Martín, F., García-Sogo, B., Angosto, T., Moreno, V., and Lozano, R. (2010). Functional analysis of the *Arlequin* mutant corroborates the essential role of the *Arlequin/TAGL1* gene during reproductive development of tomato. PLoS One **5:** e14427.

Glover, B.J. (2014). Understanding Flowers and Flowering: An Integrated Approach. (Oxford: Oxford University Press).

Goodrich, J., Carpenter, R., and Coen, E.S. (1992). A common gene regulates pigmentation pattern in diverse plant species. Cell **68:** 955–964.

Grotewold, E., and Davies, K. (2008). Trafficking and sequestration of anthocyanins. Nat. Prod. Commun. **3:** 1251–1258.

Hiesey, W.M., Nobs, M.A., and Björkman, O. (1971). Experimental studies on the nature of species. V. Biosystematics, genetics, and physiological ecology of the Erythranthe section of Mimulus. In Carnegie Institute of Washington Publication, Volume **628, pp.** 1–213.

Itkin, M., Seybold, H., Breitel, D., Rogachev, I., Meir, S., and Aharoni, A. (2009). TOMATO AGAMOUS-LIKE 1 is a component of the fruit ripening regulatory network. Plant J. **60:** 1081–1095.

Ito, Y., Kitagawa, M., Ihashi, N., Yabe, K., Kimbara, J., Yasuda, J., Ito, H., Inakuma, T., Hiroi, S., and Kasumi, T. (2008). DNA-binding specificity, transcriptional activation potential, and the *rin* mutation effect for the tomato fruit-ripening regulator RIN. Plant J. **55:** 212–223.

Karlova, R., Rosin, F.M., Busscher-Lange, J., Parapunova, V., Do, P.T., Fernie, A.R., Fraser, P.D., Baxter, C., Angenent, G.C., and de Maagd, R.A. (2011). Transcriptome and metabolite profiling show that APETALA2a is a major regulator of tomato fruit ripening. Plant Cell **23:** 923–941.

Kerschen, A., Napoli, C.A., Jorgensen, R.A., and Müller, A.E. (2004). Effectiveness of RNA interference in transgenic plants. FEBS Lett. **566:** 223–228.

Kolotilin, I., Koltai, H., Tadmor, Y., Bar-Or, C., Reuveni, M., Meir, A., Nahon, S., Shlomo, H., Chen, L., and Levin, I. (2007). Transcriptional profiling of high pigment-2dg tomato mutant links early fruit plastid biogenesis with its overproduction of phytonutrients. Plant Physiol. **145:** 389–401.

Kozlov, A.M., Darriba, D., Flouri, T., Morel, B., and Stamatakis, A. (2019). RAxML-NG: A fast, scalable and user-friendly tool for maximum likelihood phylogenetic inference. Bioinformatics **35:** 4453–4455.

Larkin, R.M., Stefano, G., Ruckle, M.E., Stavoe, A.K., Sinkler, C.A., Brandizzi, F., Malmstrom, C.M., and Osteryoung, K.W. (2016). *REDUCED CHLOROPLAST COVERAGE* genes from *Arabidopsis thaliana* help to establish the size of the chloroplast compartment. Proc. Natl. Acad. Sci. USA **113:** E1116–E1125.

Li, L., Paolillo, D.J., Parthasarathy, M.V., Dimuzio, E.M., and Garvin, D.F. (2001). A novel gene mutation that confers abnormal patterns of β-carotene accumulation in cauliflower (*Brassica oleracea* var. *botrytis*). Plant J. **26:** 59–67.

Li, L., and Yuan, H. (2013). Chromoplast biogenesis and carotenoid accumulation. Arch. Biochem. Biophys. **539:** 102–109.

Lichtenthaler, H.K. (1987). Chlorophyll and carotenoids: Pigments of photosynthetic biomembranes. Methods Enzymol. **148:** 350–382.

Liu, Y., Roof, S., Ye, Z., Barry, C., van Tuinen, A., Vrebalov, J., Bowler, C., and Giovannoni, J. (2004a). Manipulation of light signal transduction as a means of modifying fruit nutritional quality in tomato. Proc. Natl. Acad. Sci. USA **101:** 9897–9902.

Liu, Z., Yan, H., Wang, K., Kuang, T., Zhang, J., Gui, L., An, X., and Chang, W. (2004b). Crystal structure of spinach major light-harvesting complex at 2.72 A resolution. Nature **428:** 287–292.

Llorente, B., D'Andrea, L., Ruiz-Sola, M.A., Botterweg, E., Pulido, P., Andilla, J., Loza-Alvarez, P., and Rodriguez-Concepcion, M. (2016). Tomato fruit carotenoid biosynthesis is adjusted to actual ripening progression by a light-dependent mechanism. Plant J. **85:** 107–119.

Logan, D.C., Scott, I., and Tobin, A.K. (2003). The genetic control of plant mitochondrial morphology and dynamics. Plant J. **36:** 500–509.

Lopez, A.B., Van Eck, J., Conlin, B.J., Paolillo, D.J., O'Neill, J., and Li, L. (2008). Effect of the cauliflower *Or* transgene on carotenoid accumulation and chromoplast formation in transgenic potato tubers. J. Exp. Bot. **59:** 213–223.

Lu, S., et al. (2006). The cauliflower Or gene encodes a DnaJ cysteine-rich domain-containing protein that mediates high levels of β-carotene accumulation. Plant Cell **18:** 3594–3605.

Lu, S., Zhang, Y., Zhu, K., Yang, W., Ye, J., Chai, L., Xu, Q., and Deng, X. (2018). The citrus transcription factor CsMADS6 modulates carotenoid metabolism by directly regulating carotenogenic genes. Plant Physiol. **176:** 2657–2676.

Ludwig, S.R., Habera, L.F., Dellaporta, S.L., and Wessler, S.R. (1989). Lc, a member of the maize R gene family responsible for tissue-specific anthocyanin production, encodes a protein similar to transcriptional activators and contains the myc-homology region. Proc. Natl. Acad. Sci. USA **86:** 7092–7096.

Lunch, C.K., Lafountain, A.M., Thomas, S., Frank, H.A., Lewis, L.A., and Cardon, Z.G. (2013). The xanthophyll cycle and NPQ in diverse desert and aquatic green algae. Photosynth. Res. **115:** 139–151.

Ma, N., Feng, H., Meng, X., Li, D., Yang, D., Wu, C., and Meng, Q. (2014). Overexpression of tomato SlNAC1 transcription factor alters fruit pigmentation and softening. BMC Plant Biol. **14:** 351.

Marchler-Bauer, A., et al. (2015). CDD: NCBI's conserved domain database. Nucleic Acids Res. **43:** D222–D226.

Martel, C., Vrebalov, J., Tafelmeyer, P., and Giovannoni, J.J. (2011). The tomato MADS-box transcription factor RIPENING INHIBITOR interacts with promoters involved in numerous ripening processes in a COLORLESS NONRIPENING-dependent manner. Plant Physiol. **157:** 1568–1579.

Martin, C., Prescott, A., Mackay, S., Bartlett, J., and Vrijlandt, E. (1991). Control of anthocyanin biosynthesis in flowers of *Antirrhinum majus*. Plant J. **1:** 37–49.

Martins, T.R., Jiang, P., and Rausher, M.D. (2017). How petals change their spots: cis-regulatory re-wiring in *Clarkia* (Onagraceae). New Phytol. **216:** 510–518.

Meier, S., Tzfadia, O., Vallabhaneni, R., Gehring, C., and Wurtzel, E.T. (2011). A transcriptional analysis of carotenoid, chlorophyll and plastidial isoprenoid biosynthesis genes during development and osmotic stress responses in *Arabidopsis thaliana*. BMC Syst. Biol. **5:** 77.

Meng, C., Yang, D., Ma, X., Zhao, W., Liang, X., Ma, N., and Meng, Q. (2016). Suppression of tomato SlNAC1 transcription factor delays fruit ripening. J. Plant Physiol. **193:** 88–96.

Meng, Y., Wang, Z., Wang, Y., Wang, C., Zhu, B., Liu, H., Ji, W., Wen, J., Chu, C., Tadege, M., Niu, L., and Lin, H. (2019). The MYB activator WHITE PETAL1 associates with MtTT8 and MtWD40–1 to regulate carotenoid-derived flower pigmentation in *Medicago truncatula*. Plant Cell **31:** 2751–2767.

Mustilli, A.C., Fenzi, F., Ciliento, R., Alfano, F., and Bowler, C. (1999). Phenotype of the tomato *high pigment-2* mutant is caused by a mutation in the tomato homolog of *DEETIOLATED1*. Plant Cell **11:** 145–157.

Nisar, N., Li, L., Lu, S., Khin, N.C., and Pogson, B.J. (2015). Carotenoid metabolism in plants. Mol. Plant **8:** 68–82.

Ohmiya, A., Kishimoto, S., Aida, R., Yoshioka, S., and Sumitomo, K. (2006). Carotenoid cleavage dioxygenase (CmCCD4a) contributes to white color formation in chrysanthemum petals. Plant Physiol. **142:** 1193–1201.

Osteryoung, K.W., and Pyke, K.A. (2014). Division and dynamic morphology of plastids. Annu. Rev. Plant Biol. **65:** 443–472.

Owen, C.R., and Bradshaw, H.D. (2011). Induced mutations affecting pollinator choice in *Mimulus lewisii* (Phrymaceae). Arthropod Plant Interact. **5:** 235–244.

Paz-Ares, J., Ghosal, D., Wienand, U., Peterson, P.A., and Saedler, H. (1987). The regulatory c1 locus of *Zea mays* encodes a protein with homology to myb proto-oncogene products and with structural similarities to transcriptional activators. EMBO J. **6:** 3553–3558.

Pyke, K. (2011). Analysis of plastid number, size, and distribution in Arabidopsis plants by light and fluorescence microscopy. In Methods Mol. Biol., Volume **774, pp.** 19–32.

Qin, G., Wang, Y., Cao, B., Wang, W., and Tian, S. (2012). Unraveling the regulatory network of the MADS box transcription factor RIN in fruit ripening. Plant J. **70:** 243–255.

Quattrocchio, F., Wing, J.F., van der Woude, K., Mol, J.N.M., and Koes, R. (1998). Analysis of bHLH and MYB domain proteins: Species-specific regulatory differences are caused by divergent evolution of target anthocyanin genes. Plant J. **13:** 475–488.

Ruiz-Sola, M., and Rodríguez-Concepción, M. (2012). Carotenoid biosynthesis in Arabidopsis: A colorful pathway. Arabidopsis Book **10:** e0158.

Sagawa, J.M., Stanley, L.E., LaFountain, A.M., Frank, H.A., Liu, C., and Yuan, Y.-W. (2016). An R2R3-MYB transcription factor regulates carotenoid pigmentation in *Mimulus lewisii* flowers. New Phytol. **209:** 1049–1057.

Schwinn, K., Venail, J., Shang, Y., Mackay, S., Alm, V., Butelli, E., Oyama, R., Bailey, P., Davies, K., and Martin, C. (2006). A small family of MYB-regulatory genes controls floral pigmentation intensity and patterning in the genus *Antirrhinum*. Plant Cell **18:** 831–851.

Shang, Y., Venail, J., Mackay, S., Bailey, P.C., Schwinn, K.E., Jameson, P.E., Martin, C.R., and Davies, K.M. (2011). The molecular basis for venation patterning of pigmentation and its effect on pollinator attraction in flowers of *Antirrhinum*. New Phytol. **189:** 602–615.

Shima, Y., Kitagawa, M., Fujisawa, M., Nakano, T., Kato, H., Kimbara, J., Kasumi, T., and Ito, Y. (2013). Tomato FRUITFULL homologues act in fruit ripening via forming MADS-box transcription factor complexes with RIN. Plant Mol. Biol. **82:** 427–438.

Spelt, C., Quattrocchio, F., Mol, J.N.M., and Koes, R. (2000). anthocyanin1 of petunia encodes a basic helix-loop-helix protein that directly activates transcription of structural anthocyanin genes. Plant Cell **12:** 1619–1632.

Sun, T., and Li, L. (2020). Toward the 'golden' era: The status in uncovering the regulatory control of carotenoid accumulation in plants. Plant Sci. **290:** 110331.

Toledo-Ortiz, G., Huq, E., and Rodríguez-Concepción, M. (2010). Direct regulation of phytoene synthase gene expression and carotenoid biosynthesis by phytochrome-interacting factors. Proc. Natl. Acad. Sci. USA **107:** 11626–11631.

Toledo-Ortiz, G., Johansson, H., Lee, K.P., Bou-Torrent, J., Stewart, K., Steel, G., Rodríguez-Concepción, M., and Halliday, K.J. (2014). The HY5-PIF regulatory module coordinates light and temperature control of photosynthetic gene transcription. PLoS Genet. **10:** e1004416.

Tseng, T.S., Swain, S.M., and Olszewski, N.E. (2001). Ectopic expression of the tetratricopeptide repeat domain of SPINDLY causes defects in gibberellin response. Plant Physiol. **126:** 1250–1258.

Tzuri, G., et al. (2015). A 'golden' SNP in *CmOr* governs the fruit flesh color of melon (*Cucumis melo*). Plant J. **82:** 267–279.

Vrebalov, J., Pan, I.L., Arroyo, A.J.M., McQuinn, R., Chung, M., Poole, M., Rose, J., Seymour, G., Grandillo, S., Giovannoni, J., and Irish, V.F. (2009). Fleshy fruit expansion and ripening are regulated by the Tomato SHATTERPROOF gene TAGL1. Plant Cell **21:** 3041–3062.

Vrebalov, J., Ruezinsky, D., Padmanabhan, V., White, R., Medrano, D., Drake, R., Schuch, W., and Giovannoni, J. (2002). A MADS-box gene necessary for fruit ripening at the tomato *ripening-inhibitor* (*rin*) locus. Science **296:** 343–346.

Welsch, R., Maass, D., Voegel, T., Dellapenna, D., and Beyer, P. (2007). Transcription factor RAP2.2 and its interacting partner SINAT2: stable elements in the carotenogenesis of *Arabidopsis* leaves. Plant Physiol. **145:** 1073–1085.

Xiong, C., et al. (2019). A tomato B-box protein SlBBX20 modulates carotenoid biosynthesis by directly activating PHYTOENE SYNTHASE 1, and is targeted for 26S proteasome-mediated degradation. New Phytol. **221:** 279–294.

Xu, W., Dubos, C., and Lepiniec, L. (2015). Transcriptional control of flavonoid biosynthesis by MYB-bHLH-WDR complexes. Trends Plant Sci. **20:** 176–185.

Yuan, H., Zhang, J., Nageswaran, D., and Li, L. (2015). Carotenoid metabolism and regulation in horticultural crops. Hortic. Res. **2:** 15036.

Yuan, Y.-W., Sagawa, J.M., Di Stilio, V.S., and Bradshaw, H.D., Jr. (2013a). Bulk segregant analysis of an induced floral mutant identifies a MIXTA-like R2R3 MYB controlling nectar guide formation in *Mimulus lewisii*. Genetics **194:** 523–528.

Yuan, Y.-W., Sagawa, J.M., Frost, L., Vela, J.P., and Bradshaw, H.D., Jr. (2014). Transcriptional control of floral anthocyanin pigmentation in monkeyflowers (*Mimulus*). New Phytol. **204:** 1013–1027.

Yuan, Y.-W., Sagawa, J.M., Young, R.C., Christensen, B.J., and Bradshaw, H.D., Jr. (2013b). Genetic dissection of a major anthocyanin QTL contributing to pollinator-mediated reproductive isolation between sister species of *Mimulus*. Genetics **194:** 255–263.

Zeytuni, N., and Zarivach, R. (2012). Structural and functional discussion of the tetra-trico-peptide repeat, a protein interaction module. Structure **20:** 397–405.

Zhang, B., Liu, C., Wang, Y., Yao, X., Wang, F., Wu, J., King, G.J., and Liu, K. (2015). Disruption of a CAROTENOID CLEAVAGE

DIOXYGENASE 4 gene converts flower colour from white to yellow in *Brassica* species. New Phytol. **206:** 1513–1526.

Zhong, S., Fei, Z., Chen, Y.R., Zheng, Y., Huang, M., Vrebalov, J., McQuinn, R., Gapper, N., Liu, B., Xiang, J., Shao, Y., and Giovannoni, J.J. (2013). Single-base resolution methylomes of tomato fruit development reveal epigenome modifications associated with ripening. Nat. Biotechnol. **31:** 154–159.

Zhou, D., Shen, Y., Zhou, P., Fatima, M., Lin, J., Yue, J., Zhang, X., Chen, L.Y., and Ming, R. (2019). Papaya *CpbHLH1/2* regulate carotenoid biosynthesis-related genes during papaya fruit ripening. Hortic. Res. **6:** 80.

Zhou, X., Welsch, R., Yang, Y., Álvarez, D., Riediger, M., Yuan, H., Fish, T., Liu, J., Thannhauser, T.W., and Li, L. (2015). Arabidopsis OR proteins are the major posttranscriptional regulators of phytoene synthase in controlling carotenoid biosynthesis. Proc. Natl. Acad. Sci. USA **112:** 3558–3563.

Zhu, F., et al. (2017). An R2R3-MYB transcription factor represses the transformation of α- and β-branch carotenoids by negatively regulating expression of *CrBCH2* and *CrNCED5* in flavedo of *Citrus reticulate*. New Phytol. **216:** 178–192.

Zhu, M., Chen, G., Zhang, J., Zhang, Y., Xie, Q., Zhao, Z., Pan, Y., and Hu, Z. (2014). The abiotic stress-responsive NAC-type transcription factor SlNAC4 regulates salt and drought tolerance and stress-related genes in tomato (*Solanum lycopersicum*). Plant Cell Rep. **33:** 1851–1863.

Zhu, Q., Hulen, D., Liu, T., and Clarke, M. (1997). The *cluA*- mutant of *Dictyostelium* identifies a novel class of proteins required for dispersion of mitochondria. Proc. Natl. Acad. Sci. USA **94:** 7308–7313.